Article

Intramolecular NH···S Hydrogen Bonding in the Zinc Thiolate Complex [Tm]ZnSCHC(O)NHPh: A Mechanistic Investigation of Thiolate Alkylation as Probed by Kinetics Studies and by Kinetic Isotope Effects

Melissa M. Morlok, Kevin E. Janak, Guang Zhu, Duncan A. Quarless, and Gerard Parkin

J. Am. Chem. Soc., **2005**, 127 (40), 14039-14050• DOI: 10.1021/ja0536670 • Publication Date (Web): 17 September 2005

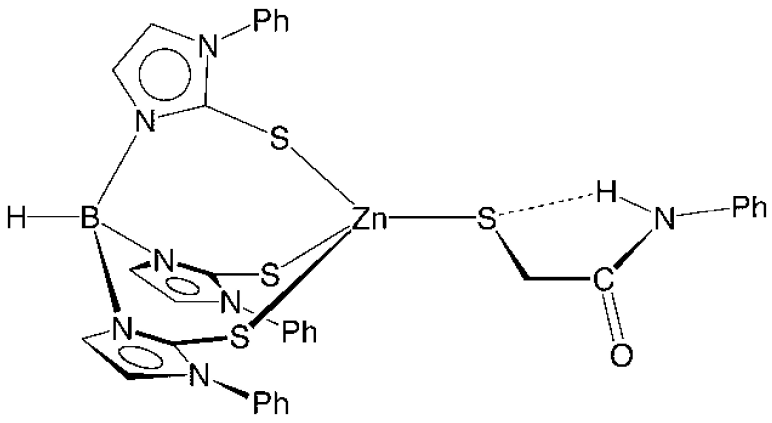

More About This Article

Additional resources and features associated with this article are available within the HTML version:

- Supporting Information
- Links to the 5 articles that cite this article, as of the time of this article download
- Access to high resolution figures
- Links to articles and content related to this article
- Copyright permission to reproduce figures and/or text from this article

View the Full Text HTML

J|A|C|S
ARTICLES
Published on Web 09/17/2005

Intramolecular N−H···S Hydrogen Bonding in the Zinc Thiolate Complex [Tm^{Ph}]ZnSCH$_2$C(O)NHPh: A Mechanistic Investigation of Thiolate Alkylation as Probed by Kinetics Studies and by Kinetic Isotope Effects

Melissa M. Morlok, Kevin E. Janak, Guang Zhu, Duncan A. Quarless, and Gerard Parkin*

Contribution from the Department of Chemistry, Columbia University, New York, New York 10027

Received June 3, 2005; E-mail: parkin@chem.columbia.edu

Abstract: The zinc thiolate complex [Tm^{Ph}]ZnSCH$_2$C(O)N(H)Ph, which features a tetrahedral [ZnS$_4$] motif analogous to that of the Ada DNA repair protein, may be obtained by the reaction of Zn(NO$_3$)$_2$ with [Tm^{Ph}]Li and Li[SCH$_2$C(O)N(H)Ph] ([Tm^{Ph}] = tris(2-mercapto-1-phenylimidazolyl)hydroborato ligand). Structural characterization of [Tm^{Ph}]ZnSCH$_2$C(O)N(H)Ph by X-ray diffraction demonstrates that the molecule exhibits an intramolecular N−H···S hydrogen bond between the amide N−H group and thiolate sulfur atom, a structure that is reproduced by density functional theory (DFT) calculations. The thiolate ligand of [Tm^{Ph}]ZnSCH$_2$C(O)N(H)Ph is subject to alkylation, a reaction that is analogous to the function of the Ada DNA repair protein. Specifically, [Tm^{Ph}]ZnSCH$_2$C(O)N(H)Ph reacts with MeI to yield PhN(H)C(O)CH$_2$SMe and [Tm^{Ph}]ZnI, a reaction which is characterized by second-order kinetics that is consistent with either (i) an associative mechanism or (ii) a stepwise dissociative mechanism in which the alkylation step is rate determining. Although the kinetics studies are incapable of distinguishing between these possibilities, a small normal kinetic isotope effect of $k_H/k_D = 1.16(1)$ at 0 °C for the reaction of [Tm^{Ph}]ZnSCH$_2$C(O)N(**H***)Ph (**H*** = H, D) with MeI is suggestive of a dissociative mechanism on the basis of DFT calculations. In particular, DFT calculations demonstrate that a normal kinetic isotope effect requires thiolate dissociation because it results in the formation of [PhN(H)C(O)CH$_2$S]$^-$ which, as an anion, exhibits a stronger N−H···S hydrogen bonding interaction than that in [Tm^{Ph}]ZnSCH$_2$C(O)N(H)Ph. Correspondingly, mechanisms that involve direct alkylation of coordinated thiolate are predicted to be characterized by $k_H/k_D \leq 1$ because the reaction involves a reduction of the negative charge on sulfur and hence a weakening of the N−H···S hydrogen bonding interaction.

Introduction

Zinc plays a variety of structural and functional roles in biological systems.[1,2] While the geometries of the zinc centers in both structural and functional sites are commonly tetrahedral, a long held distinction between the two types of sites was the presence of a water molecule, the essential catalytic component, at the functional site. More recently, however, a class of zinc proteins and enzymes with tetrahedral non-aqua functional zinc sites has started to emerge in which the activity centers on the reactivity of a zinc−thiolate linkage rather than that of a zinc−aqua or hydroxide ligand. For example, alkylation of zinc−cysteine thiolates is involved in the mechanisms of action of several enzymes and proteins, of which the first to be discovered was the Ada DNA repair protein with a tetrahedral [(Cys)$_4$Zn] active site.[3−5] This reactivity of the zinc−cysteine thiolate

(1) (a) Vallee, B. L.; Auld, D. S. *Acc. Chem. Res.* **1993**, *26*, 543−551. (b) Auld, D. S. *Struct. Bonding (Berlin)* **1997**, *89*, 29−50. (c) Coleman, J. E. *Curr. Opin. Chem. Biol.* **1998**, *2*, 222−234. (d) Rahuel-Clermont, S.; Dunn, M. F. *Copper Zinc Inflammatory Degener. Dis.* **1998**, 47−59. (e) Holm, R. H.; Kennepohl, P.; Solomon, E. I. *Chem. Rev.* **1996**, *96*, 2239−2314. (f) Lipscomb, W. N.; Sträter, N. *Chem. Rev.* **1996**, *96*, 2375−2433. (g) Lindskog, S. *Pharmacol. Ther.* **1997**, *74*, 1−20.

(2) (a) Parkin, G. *Chem. Rev.* **2004**, *104*, 699−767. (b) Parkin, G. *Chem. Commun.* **2000**, 1971−1985. (c) Parkin, G. *Metal Ions in Biological Systems*; Sigel, A., Sigel, H., Eds.; Marcel Dekker: New York, 2001; Vol. 38, Ch. 14, pp 411−460.

(3) (a) Myers, L. C.; Terranova, M. P.; Ferentz, A. E.; Wagner, G.; Verdine, G. L. *Science* **1993**, *261*, 1164−1167. (b) Myers, L. C.; Jackow, F.; Verdine, G. L. *J. Biol. Chem.* **1995**, *270*, 6664−6670.

(4) Other zinc proteins that involve zinc−thiolate alkylation in their mechanisms of action include methionine synthase, methanol-coenzyme M methyltransferase, farnesyl-protein transferase, and geranylgeranyl-protein transferase. See (a) Matthews, R. G.; Goulding, C. W. *Curr. Opin. Chem. Biol.* **1997**, *1*, 332−339. (b) Hightower, K. E.; Fierke, C. A. *Curr. Opin. Chem. Biol.* **1999**, *3*, 176−181. (c) Strickland, C. L.; Weber, P. C. *Curr. Opin. Drug Discovery Dev.* **1999**, *2*, 475−483. (d) Penner-Hahn, J. E. Zn catalyzed alkyl-transfer reactions: A new class of biological Zn sites. *Indian J. Chem., Sect. A* **2002**, *41*, 13-21. (e) Matthews, R. G. *Acc. Chem. Res.* **2001**, *34*, 681−689. (f) Harris, C. M.; Poulter, C. D. *Nat. Prod. Rep.* **2000**, *17*, 137−144. (g) McCall, K. A.; Huang, C.-C.; Fierke, C. A. *J. Nutr.* **2000**, *130*, 1437S−1446S.

(5) In addition to alkylation, proteolytic cleavage of zinc−thiolate groups is also of relevance, as illustrated by the matrix metalloproteinases (matrixins), a class of enzymes that are essential for embryonic development, wound healing, bone and growth development, and other physiological remodeling processes. See, for example, (a) Borkakoti, N. *Curr. Opin. Drug Discovery Dev.* **1999**, *2*, 449−462. (b) Bode, W.; Fernandez-Catalan, C.; Tschesche, H.; Grams, F.; Nagase, H.; Maskos, K. *Cell. Mol. Life Sci.* **1999**, *55*, 639−652. (c) Nagase, H.; Woessner, J. F., Jr. *J. Biol. Chem.* **1999**, *274*, 21491−21494. (d) Stöcker, W.; Grams, F.; Baumann, U.; Reinemer, P.; Gomis-Rüth, F.-X.; McKay, D. B.; Bode, W. *Protein Sci.* **1995**, *4*, 823−40.

moiety is particularly interesting in view of the otherwise inert nature when it is a component of a structural site, as exemplified by the [$Cys_{\alpha}His_{\beta}Zn$] ($\alpha + \beta = 4$) motifs of zinc fingers.[1,6,7] An appreciation of the factors responsible for dictating whether a given zinc−cysteine thiolate linkage provides a structural or functional role is paramount for understanding fully the biological role of zinc. In this regard, while it is recognized that hydrogen bonding interactions involving sulfur as an acceptor are weaker than those involving oxygen,[8] their importance in influencing chemistry has, nevertheless, been considered for a variety of other systems,[9] and it has been postulated that N−H···S hydrogen bonding interactions between thiolate sulfur and amide groups of other residues provide a mechanism to modulate the reactivity of the zinc−cysteine thiolate moiety.[7,10,11] In this paper, we report (i) the synthesis and structural characterization of a tetrahedral zinc thiolate complex that features an intramolecular N−H···S hydrogen bond and (ii) studies to evaluate the mechanism of thiolate alkylation.

Results and Discussion

We have previously employed the tris(2-mercapto-1-arylimidazolyl)hydroborato ligand system, [Tm^{Ar}], to provide an [S_3]-donor array that provides a stable platform for investigating chemistry relevant to zinc enzymes and proteins with sulfur-rich active sites.[12−15] For example, the active site of the Ada DNA repair protein exhibits a [Cys_4Zn] motif, as do the structural sites in many other zinc proteins and enzymes. Structurally characterized examples of mononuclear complexes with tetrahedral [S_4Zn] motifs are not, however, well-precedented. Furthermore, the only examples of [S_4Zn] complexes that incorporate thiolate ligands are arylthiolate derivatives, namely, $[Zn(SAr)_4]^{2-}$,[16−18] [Tm^{Ph}]ZnSPh,[12,15a] and [$PhB(CH_2SBu^t)_3$]-ZnSPh.[19,20] In an effort to provide an improved structural and functional model for the active site of Ada, we sought to synthesize derivatives in which the thiolate more closely resembles cysteine thiolate. However, since the application of cysteine itself to prepare complexes with $Zn-SCH_2X$ bonds [$X = CH(CO_2^-)(NH_3^+)$] is not well-established,[21,22] possibly a consequence of the noninnocent nature of the amino acid groups,[23] we have attempted to synthesize other analogues. In particular, we have focused on the use of *N*-phenyl-2-mercaptoacetamide [$PhN(H)C(O)CH_2SH$],[24] which also incorporates a potential hydrogen bonding N−H group.

Synthesis and Structural Characterization of [Tm^{Ph}]-$ZnSCH_2C(O)N(H)Ph$. The thiolate complex [Tm^{Ph}]$ZnSCH_2C(O)N(H)Ph$ may be readily obtained by the reaction of $Zn(NO_3)_2$ with [Tm^{Ph}]Li and Li[$SCH_2C(O)N(H)Ph$] (Scheme 1). [Tm^{Ph}]-$ZnSCH_2C(O)N(H)Ph$ has been obtained in two different crystalline forms of composition [Tm^{Ph}]$ZnSCH_2C(O)N(H)Ph$ and [Tm^{Ph}]$ZnSCH_2C(O)N(H)Ph\cdot1.5EtOH$ by crystallization from chloroform and ethanol, respectively, both of which have been structurally characterized by single-crystal X-ray diffraction. As illustrated in Figures 1 and 2, the zinc coordination environments within the two crystalline forms are similar, even though the two structures differ by the presence of an O−H···O hydrogen bonding interaction between the carbonyl oxygen of the amide group and the hydroxy group of an ethanol molecule [$d(O\cdots O) = 2.786(3)$ Å]. Comparison of the bond length data in Table 1, however, indicates that the O−H···O hydrogen bond exerts little influence on the metrical parameters of the zinc center. Furthermore, the $Zn-SCH_2C(O)N(H)Ph$ bond lengths in the two forms of [Tm^{Ph}]$ZnSCH_2C(O)N(H)Ph$ [2.284(1) and 2.267(1) Å] are comparable to the Zn−SPh bond length in [Tm^{Ph}]ZnSPh [2.258(1) Å].[12] These Zn−SR bond lengths are shorter than the

(6) (a) Maret, W. *Biochemistry* **2004**, *43*, 3301−3309. (b) Iuchi, S. *Cell. Mol. Life Sci.* **2001**, *58*, 625−635. (c) Berg, J. M.; Shi, Y. *Science* **1996**, *271*, 1081−1085. (d) Laity, J. H.; Lee, B. M.; Wright, P. E. *Curr. Opin. Struct. Biol.* **2001**, *11*, 39−46. (e) Berg, J. M.; Godwin, H. A. *Annu. Rev. Biophys. Biomol. Struct.* **1997**, *26*, 357−371.

(7) Maynard, A. T.; Covell, D. G. *J. Am. Chem. Soc.* **2001**, *123*, 1047−1058.

(8) (a) Platts, J. A.; Howard, S. T.; Bracke, B. R. F. *J. Am. Chem. Soc.* **1996**, *118*, 2726−2733. (b) Sennikov, P. G. *J. Phys. Chem.* **1994**, *98*, 4973−4981.

(9) See, for example, (a) Okamura, T.-A.; Takamizawa, S.; Ueyama, N.; Nakamura, A. *Inorg. Chem.* **1998**, *37*, 18−28. (b) François, S.; Rohmer, M. M.; Bénard, M.; Moreland, A. C.; Rauchfuss, T. B. *J. Am. Chem. Soc.* **2000**, *122*, 12743−12750. (c) McGuire, D. G.; Khan, M. A.; Ashby, M. T. *Inorg. Chem.* **2002**, *41*, 2202−2208 and references therein. (d) Conry, R. R.; Tipton, A. A. *J. Biol. Inorg. Chem.* **2001**, *6*, 359−366. (e) Huang, J.; Dewan, J. C.; Walters, M. A. *Inorg. Chim. Acta* **1995**, *228*, 199−206. (f) Ueyama, N.; Taniuchi, K.; Okamura, T.; Nakamura, A.; Maeda, H.; Emura, S. *Inorg. Chem.* **1996**, *35*, 1945−1951. (g) Ueyama, N.; Okamura, T. A.; Nakamura, A. *J. Am. Chem. Soc.* **1992**, *114*, 8129−8137.

(10) (a) Karlin, S.; Zhu, Z.-Y. *Proc. Natl. Acad. Sci. U.S.A.* **1997**, *94*, 14231−14236. (b) Simonson, T.; Calimet, N. *Proteins* **2002**, *49*, 37−48. (c) Dudev, T.; Lim, C. *J. Am. Chem. Soc.* **2002**, *124*, 6759−6766.

(11) Myers, L. C.; Verdine, G. L.; Wagner, G. *Biochemistry* **1993**, *32*, 2, 14089−14094.

(12) Bridgewater, B. M.; Fillebeen, T.; Friesner, R. A.; Parkin, G. *J. Chem. Soc., Dalton Trans.* **2000**, 4494−4496.

(13) (a) Kimblin, C.; Bridgewater, B. M.; Churchill, D. G.; Parkin, G. *Chem. Commun.* **1999**, 2301−2302. (b) Bridgewater, B. M.; Parkin, G. *J. Am. Chem. Soc.* **2000**, *122*, 7140−7141. (c) Bridgewater, B. M.; Parkin, G. *Inorg. Chem. Commun.* **2001**, *4*, 126−129.

(14) (a) Docrat, A.; Morlok, M. M.; Bridgewater, B. M.; Churchill, D. G.; Parkin, G. *Polyhedron* **2004**, *23*, 481−488. (b) Morlok, M. M.; Docrat, A.; Janak, K. E.; Tanski, J. M.; Parkin, G. *Dalton Trans.* **2004**, 3448−3452.

(15) For other recent studies on a series of [Tm^R]ZnX complexes, see (a) Melnick, J. G.; Docrat, A.; Parkin, G. *Chem. Commun.* **2004**, 2870−2871. (b) Ibrahim, M. M.; Shu, M.; Vahrenkamp, H. *Eur. J. Inorg. Chem.* **2005**, 1388−1397 and references therein.

(16) (a) Swenson, D.; Baenziger, N. C.; Coucouvanis, D. *J. Am. Chem. Soc.* **1978**, *100*, 1932−1934. (b) Ueyama, N.; Sugawara, T.; Sasaki, K.; Nakamura, A.; Yamashita, S.; Wakatsnki, Y.; Yamazaki, H.; Yasuoka, N. *Inorg. Chem.* **1988**, *27*, 741−747. (c) Coucouvanis, D.; Swenson, D.; Baenziger, N. C.; Murphy, C.; Holah, D. G.; Sfarnas, N.; Simopoulos, A.; Kostikas, A. *J. Am. Chem. Soc.* **1981**, *103*, 3350−3362.

(17) (a) Silver, A.; Koch, S. A.; Millar, M. *Inorg. Chim. Acta* **1993**, *205*, 9−14. (b) Maelia, L. E.; Millar, M.; Koch, S. A. *Inorg. Chem.* **1992**, *31*, 4594−4600. (c) Koch, S. A.; Maelia, L. E.; Millar, M. *J. Am. Chem. Soc.* **1983**, *105*, 5944−5945.

(18) Otto, J.; Jolk, I.; Viland, T.; Wonnemann, R.; Krebs, B. *Inorg. Chim. Acta* **1999**, *285*, 262−268.

(19) Chiou, S.-J.; Innocent, J.; Riordan, C. G.; Lam, K.-C.; Liable-Sands, L.; Rheingold, A. L. *Inorg. Chem.* **2000**, *39*, 4347−4353.

(20) Other structurally characterized mononuclear complexes with the [S_4Zn^{II}] coordination geometry include [Bm^{Me}]$_2$Zn,[a] [Bm^{Bu^t}]$_2$Zn,[b] [η^2-Tm^{Bu^t}]$_2$Zn,[c] [(pz)Bm^{Me}]$_2$Zn,[d] [(pz$^{Ph,\ Me}$)Bm^{Me}]$_2$Zn,[e] [η^2-$Tr^{Ph,\ Me}$]$_2$Zn,[f] [(2-mercapto-1-methylimidazole)$_4$Zn]$^{2+}$,[g] [(*N*-methyl-2-thioxopyrrolidine)$_4$Zn]$^{2+}$,[h] and {η^2-[$(Me_2N)_2C(S)]_2S$}$_2$Zn.[i] (a) Kimblin, C.; Bridgewater, B. M.; Hascall, T.; Parkin, G. *J. Chem. Soc., Dalton Trans.* **2000**, 891−897. (b) Alvarez, H. M.; Tran, T. B.; Richter, M. A.; Alyounes, D. M.; Rabinovich, D.; Tanski, J. M.; Krawiec, M. *Inorg. Chem.* **2003**, *42*, 2149−2156. (c) Tesmer, M.; Shu, M.; Vahrenkamp, H. *Inorg. Chem.* **2001**, *40*, 4022−4029. (d) Kimblin, C.; Bridgewater, B. M.; Churchill, D. G.; Hascall, T.; Parkin, G. *Inorg. Chem.* **2000**, *39*, 4240−4243. (e) Shu, M. H.; Walz, R.; Wu, B.; Seebacher, J.; Vahrenkamp, H. *Eur. J. Inorg. Chem.* **2003**, 2502−2511. (f) Lanfranchi, M.; Marchiò, L.; Mora, C.; Pellinghelli, M. A. *Inorg. Chim. Acta* **2004**, *357*, 367−375. (g) Nowell, I. W.; Cox, A. G.; Raper, E. S. *Acta Crystallogr., Sect. B* **1979**, *35*, 3047−3050. (h) Wilk, A.; Hitchman, M. A.; Massa, W.; Reinen, D. *Inorg. Chem.* **1993**, *32*, 2483−2490. (i) Armstrong, K. E.; Crane, J. D.; Whittingham, M. *Inorg. Chem. Commun.* **2004**, *7*, 784−787.

(21) Indeed, Vahrenkamp has recently commented on the paucity of structurally characterized zinc−amino acid and zinc−peptide complexes. See Rombach, M.; Gelinsky, M.; Vahrenkamp, H. *Inorg. Chim. Acta* **2002**, *334*, 25−33.

(22) For some tris(pyrazolyl)hydroborato zinc complexes that incorporate protected cysteine and homocysteine derivatives, see (a) Ruf, M.; Burth, R.; Weis, K.; Vahrenkamp, H. *Chem. Ber.* **1996**, *129*, 1251−1257. (b) Brand, U.; Rombach, M.; Seebacher, J.; Vahrenkamp, H. *Inorg. Chem.* **2001**, *40*, 6151−6157.

(23) In this regard, both sulfur and nitrogen coordinate to zinc in the cysteinato derivative $Na_2[Zn(L\text{-}cys)_2]$;[a,b] furthermore, trinuclear $[Zn_3(L\text{-}HCys)_4]^{2+}$ species that involve coordination via sulfur and oxygen have also been proposed.[b] (a) Bell, P.; Sheldrick, W. S. *Z. Naturforsch. B* **1984**, *39*, 1732−1737. (b) Shindo, H.; Brown, T. L. *J. Am. Chem. Soc.* **1965**, *87*, 1904−1909.

(24) Bhandari, C. S.; Sogani, N. C.; Mahnot, U. S. *J. Prakt. Chem./Chem.-Ztg.* **1971**, *313*, 849−854.

Scheme 1

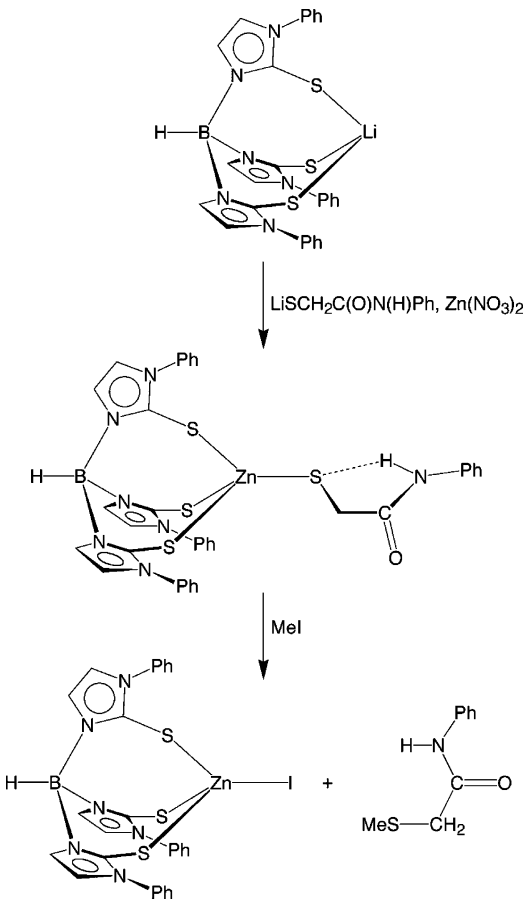

corresponding value for the related mercaptoimidazole adduct {[Tm^{Ph}]Zn(mim^{Ph})}$^+$ [2.326(1) Å],[12] consistent with a normal covalent bond description for the thiolate derivatives, [Tm^{Ph}]ZnSCH$_2$C(O)N(H)Ph and [Tm^{Ph}]ZnSPh, but a dative covalent bond description for the Zn−mim^{Ph} interaction in {[Tm^{Ph}]Zn(mim^{Ph})}$^+$.[25] Correspondingly, the Zn−SCH$_2$C(O)N(H)Ph bond lengths in the two forms of [Tm^{Ph}]ZnSCH$_2$C(O)N(H)Ph are also shorter than the Zn−S bonds pertaining to the Zn− [Tm^{Ph}] interaction, which lie in the range of 2.34−2.38 Å.

The most notable aspect of the structure of [Tm^{Ph}]ZnSCH$_2$C(O)N(H)Ph pertains to the existence of an intramolecular N−H···S hydrogen bond between the amide N−H group and the thiolate sulfur atom.[26,27] The hydrogen bonding interaction within [Tm^{Ph}]ZnSCH$_2$C(O)N(H)Ph is characterized by NH···S and N···S separations of 2.53 and 3.06 Å, respectively, while that in the ethanol adduct [Tm^{Ph}]ZnSCH$_2$C(O)N(H)Ph···O(H)Et is characterized by NH···S and N···S separations of 2.46 and 2.99 Å, respectively. For comparison, a recent analysis of the Cambridge Structural Database indicates that the mean intramolecular NH···S and N···S distances for X$_2$S derivatives are 2.60 and 3.12 Å, respectively.[28] On this basis, the N−H···S hydrogen bonding interaction within [Tm^{Ph}]ZnSCH$_2$C(O)N(H)Ph must be considered significant.[29] Furthermore, [Tm^{Ph}]ZnSCH$_2$C(O)N(H)Ph is the first example of a N−H···S hydrogen bonding interaction for a zinc complex with a tetrahedral [ZnS$_4$] geometry, although interactions of this type in zinc complexes have been previously noted for other types of complexes with arylthiolate ligands and [ZnN$_x$O$_y$S$_z$] ($x + y + z = 4$) coordination environments (e.g., Zn[S-2-C$_6$H$_4$N(H)C(O)Ph]$_2$(1-MeImH)$_2$,[30] [HC(pz^{Me_2})(C$_6$H$_2$MePr^{i}O)]ZnS[C$_6$H$_4$-*o*-NHC(O)Me],[31] [HC(pz^{Me_2})(Me$_2$CS)]ZnS[C$_6$H$_4$-*o*-NHC(O)Me,[31]

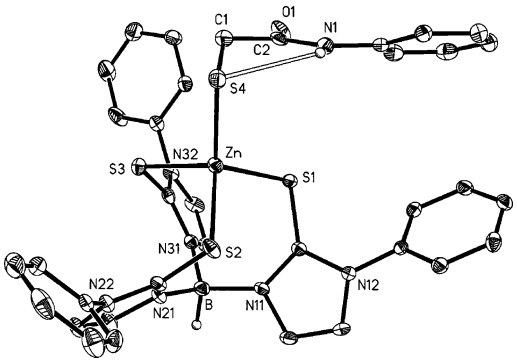

Figure 1. Molecular structure of [Tm^{Ph}]ZnSCH$_2$C(O)N(H)Ph.

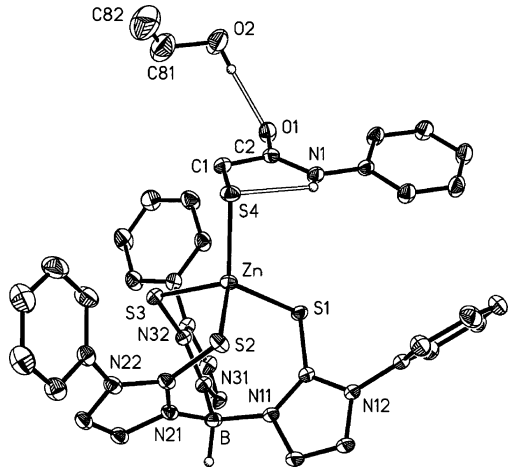

Figure 2. Molecular structure of [Tm^{Ph}]ZnSCH$_2$C(O)N(H)Ph···O(H)Et.

Table 1. Bond Length Data for [Tm^{Ph}]ZnSCH$_2$C(O)N(H)Ph and [Tm^{Ph}]ZnSCH$_2$C(O)N(H)Ph···O(H)Et

	[Tm^{Ph}]ZnSCH$_2$C(O)N(H)Ph	[Tm^{Ph}]ZnSCH$_2$C(O)N(H)Ph···O(H)Et
Zn−S(1)/Å	2.376(1)	2.359(1)
Zn−S(2)/Å	2.356(1)	2.344(1)
Zn−S(3)/Å	2.362(1)	2.361(7)
Zn−S(4)/Å	2.284(1)	2.267(1)
S(4)···H(3)/Å	2.53(4)	2.46(3)
S(4)···N(1)/Å	3.058(4)	2.987(3)
O(1)···O(2)/Å		2.786(3)

(25) For a discussion of the distinction between normal and dative covalent bonds, see Haaland, A. *Angew. Chem., Int. Ed. Engl.* **1989**, *28*, 992−1000.
(26) It is pertinent to note that spectroscopic studies have been proposed to indicate that PhN(H)C(O)CH$_2$SH possesses an intramolecular N−H···S hydrogen bond analogous to that in [Tm^{Ph}]ZnSCH$_2$C(O)N(H)Ph.[a,b] However, in the solid state, PhN(H)C(O)CH$_2$SH exists with an intermolecular N−H···O hydrogen bond.[c] (a) Bateja, S.; Chandrashekhar, S.; Bhandari, C. S.; Sogani, N. C. *J. Chin. Chem. Soc.* 1979, *26*, 173−176. (b) Bhandra, C. S.; Mehnot, U. S.; Sogani, N. C. *Bull. Acad. Pol. Sci., Ser. Sci. Chem.* 1972, *20*, 91−100. (c) See Supporting Information.
(27) An intramolecular hydrogen bond is also observed in [MeNC(O)CH$_2$S]$^-$ derivatives. See Huang, J.; Ostrander, R. L.; Rheingold, A. L.; Leung, Y.; Walters, M. A. *J. Am. Chem. Soc.* **1994**, *116*, 6769−6776.
(28) (a) Allen, F. H.; Bird, C. M.; Rowland, R. S.; Raithby, P. R. *Acta Crystallogr.* **1997**, *B53*, 696−701. (b) Allen, F. H.; Bird, C. M.; Rowland, R. S.; Raithby, P. R. *Acta Crystallogr.* **1997**, *B53*, 680−695.
(29) Furthermore, it is noteworthy that the N···S distance in [Tm^{Ph}]ZnSCH$_2$C(O)N(H)Ph is significantly shorter than a hydrogen bonding interaction involving a sulfide ligand [3.377(3) Å]. See Larsen, P. L.; Gupta, R.; Powell, D. R.; Borovik, A. S. *J. Am. Chem. Soc.* **2004**, *126*, 6522−6523.
(30) (a) Shi, X.-F.; Sun, W.-Y.; Zhang, L.; Li, C.-D. *Spectrosc. Acta, Part A* **2000**, *56*, 603−613. (b) Sun, W.-Y.; Zhang, L.; Yu, K.-B. *J. Chem. Soc., Dalton Trans.* **1999**, 795−798.

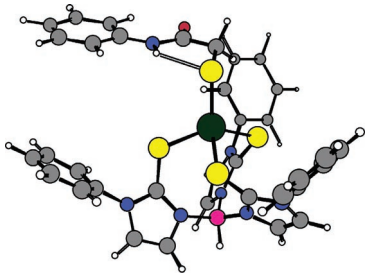

Figure 3. Geometry optimized structure of [Tm^{Ph}]ZnSCH$_2$C(O)N(H)Ph.

and [Ph(pz$^{Bu^t}$)Bt$^{Bu^t}$]ZnS[C$_6$H$_4$-*o*-NHC(O)Bu^t]).[32−34] Density functional theory (DFT) calculations reproduce well the details of the hydrogen bonding interaction within [Tm^{Ph}]ZnSCH$_2$C(O)N(H)Ph, as illustrated in Figure 3. For example, the calculated NH···S and N···S separations are 2.36 and 3.02 Å, respectively.

It is also pertinent to note that the NH···S hydrogen bonding interaction in [Tm^{Ph}]ZnSCH$_2$C(O)N(H)Ph is with the thiolate sulfur and not with one of the sulfur atoms of the [Tm^{Ph}] ligand. In this regard, calculations on {[Tm^R]Zn(mim^R)}$^+$ indicate that NH···S hydrogen bonding interactions between the N−H group of mercaptoimidazole ligands (mim^R) ligands and the sulfur atoms of a [Tm^R] ligand are feasible but are not favored relative to intermolecular N−H···O interactions with [ClO$_4$]$^-$ or MeOH acceptors.[12] Several factors are presumably responsible for the preference of the NH amide group to hydrogen bond with the thiolate sulfur of [Tm^{Ph}]ZnSCH$_2$C(O)N(H)Ph, rather than the sulfur of the [Tm^R] ligand, of which two are (i) the greater charge on the thiolate sulfur causes it to be a better hydrogen bond acceptor than a thione and (ii) hydrogen bonding to the thiolate sulfur results in a five-membered ring, whereas hydrogen bonding to the [Tm^{Ph}] sulfur results in a seven-membered ring.

Alkylation of [Tm^{Ph}]ZnSCH$_2$C(O)N(H)Ph by MeI. A key step in the mechanism of action of the Ada DNA repair protein may be modeled by the alkylation of the zinc thiolate compound [Tm^{Ph}]ZnSCH$_2$C(O)N(H)Ph. In this regard, although the Ada protein repairs DNA methylphosphotriesters, MeI has been shown to exhibit selectivity towards reaction with Cys-38 of Ada,[35] and for this reason, MeI is also a useful alkylating agent to employ in model studies. Therefore, we have investigated the reactivity of [Tm^{Ph}]ZnSCH$_2$C(O)N(H)Ph toward MeI in a chloroform solution and have observed the rapid formation of [Tm^{Ph}]ZnI[13a] and MeSCH$_2$C(O)N(H)Ph[36] (Scheme 1), thereby modeling the mechanism of action of the Ada protein.[37] In accord with previous results that indicate that the sulfur atoms of the [Tm^{Ph}] ligand are not subject to alkylation,[12,14] the observation that the sulfur atoms of the [Tm^{Ph}] ligand do not act as the hydrogen bond acceptor in [Tm^{Ph}]ZnSCH$_2$C(O)N(H)Ph provides a further indication of the different nature of the sulfur atoms in thiolate and [Tm^{Ph}] ligands. The [Tm^{Ph}] ligand thus provides a useful platform for enabling an investigation of the reactivity of a single zinc−thiolate ligand in a sulfur-rich [S$_4$Zn] coordination environment.

Scheme 2

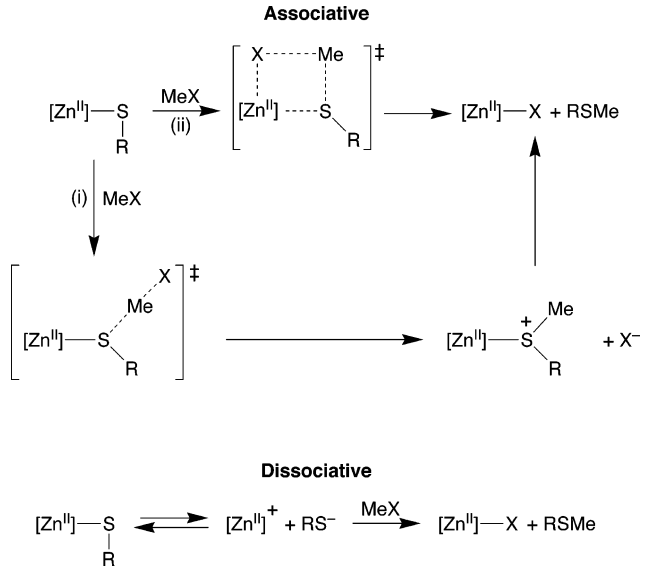

As a consequence of the important roles that zinc−thiolates play in biological systems, the alkylation of a zinc−thiolate function in simple inorganic systems has received much attention. Thus, as a result of numerous studies, it is now considered that zinc−thiolate alkylation may proceed via two mechanistic extremes that are dissociative and associative in nature. For example, (i) anionic [Zn(SPh)$_4$]$^{2-}$ is alkylated by (MeO)$_3$PO by a mechanism that is proposed to proceed via initial heterolytic dissociation generating an incipient thiolate anion,[38] while (ii) neutral derivatives such as [Tp$^{RR'}$]ZnSR,[39] [Ph(pz$^{Bu^t}$)Bt$^{Bu^t}$]ZnSAr,[19,32] [HC(pz^{Me_2})$_2$(CMe$_2$S)]ZnX,[40] [HB(mim^R)$_2$(pz)]ZnSR,[41] and a series of other zinc thiolates[31,42−46] are proposed to undergo alkylation without prior dissociation of RS$^-$ (Scheme 2). With respect to these mechanistic extremes, it is noteworthy that the transfer of a farnesyl group from farnesyl pyrophosphate to a cysteine residue mediated by protein farnesyltransferase has been proposed to involve an associative transition state.[47]

(31) (a) Smith, J. N.; Shirin, Z.; Carrano, C. J. *J. Am. Chem. Soc.* **2003**, *125*, 868−869. (b) Smith, J. N.; Hoffman, J. T.; Shirin, Z.; Carrano, C. J. *Inorg. Chem.* **2005**, *44*, 2012−2017.
(32) Chiou, S.-J.; Riordan, C. G.; Rheingold, A. L. *Proc. Natl. Acad. Sci. U.S.A.* **2003**, *100*, 3695−3700.
(33) The N···S hydrogen bond distances in these complexes are comparable to that in [Tm^{Ph}]ZnSCH$_2$C(O)N(H)Ph (e.g., Zn[S-2-C$_6$H$_4$N(H)C(O)Ph]$_2$(1-MeImH)$_2$ (2.96 Å)[30b] and [Ph(pz$^{Bu^t}$)Bt$^{Bu^t}$]ZnS[C$_6$H$_4$-*o*-NHC(O)Bu^t] (2.94 Å)[32]).
(34) On the other hand, C−H···S interactions in Zn complexes have been shown to be sufficiently weak that they do not exhibit any structure-directing properties. See Bond, A. D.; Jones, W. *J. Chem. Soc., Dalton Trans.* **2001**, 3045−3051.
(35) (a) Myers, L. C.; Wagner, G.; Verdine, G. L. *J. Am. Chem. Soc.* **1995**, *117*, 10749−10750. (b) He, C.; Wei, H.; Verdine, G. L. *J. Am. Chem. Soc.* **2003**, *125*, 1450−1451.
(36) Hellström, N.; Lauritzson, T *Chem. Ber.* **1936**, *69*, 1999−2002.
(37) [Tm^{Ph}]ZnSPh is likewise rapidly alkylated by MeI to give [Tm^{Ph}]ZnI and PhSMe. See ref 12.
(38) (a) Wilker, J. J.; Lippard, S. J. *J. Am. Chem. Soc.* **1995**, *117*, 8682−8683. (b) Wilker, J. J.; Lippard, S. J. *Inorg. Chem.* **1997**, *36*, 969−978.
(39) (a) Brand, U.; Rombach, M.; Vahrenkamp, H. *Chem. Commun.* **1998**, 2717−2718. (b) Burth, R.; Vahrenkamp, H. *Z. Anorg. Allg. Chem.* **1998**, *624*, 381−385. (c) Rombach, M.; Vahrenkamp, H. *Inorg. Chem.* **2001**, *40*, 6144−6150 (d) Ref 22b.
(40) (a) Hammes, B. S.; Carrano, C. J. *Chem. Commun.* **2000**, 1635−1636. (b) Hammes, B. S.; Carrano, C. J. *Inorg. Chem.* **2001**, *40*, 919−927.
(41) Ji, M.; Benkmil, B.; Vahrenkamp, H. *Inorg. Chem.* **2005**, *44*, 3518−3523.
(42) Hammes, B. S.; Carrano, C. J. *Inorg. Chem.* **1999**, *38*, 4593−4600.
(43) Warthen, C. R.; Hammes, B. S.; Carrano, C. J.; Crans, D. C. *J. Biol. Inorg. Chem.* **2001**, *6*, 82−90.
(44) (a) Seebacher, J.; Ji, M.; Vahrenkamp, H. *Eur. J. Inorg. Chem.* **2004**, 409−417. (b) Ji, M.; Vahrenkamp, H. *Eur. J. Inorg. Chem.* **2005**, 1398−1405.
(45) Fox, D. C.; Fiedler, A. T.; Halfen, H. L.; Brunold, T. C.; Halfen, J. A. *J. Am. Chem. Soc.* **2004**, *126*, 7627−7638.
(46) Additional studies involving methylation of a chelated thiolate ligand with MeI suggest that the issue of whether alkylation occurs at a zinc-bound thiolate or a dissociated thiolate is still a matter of debate. See Grapperhaus, C. A.; Tuntulani, T.; Reibenspies, J. H.; Darensbourg, M. Y. *Inorg. Chem.* **1998**, *37*, 4052−4058.
(47) Huang, C. C.; Hightower, K. E.; Fierke, C. A. *Biochemistry* **2000**, *39*, 2593−2602.

In view of the fact that two different mechanisms have been proposed for alkylation of a zinc thiolate ligand, we have performed a series of kinetics studies in an attempt to discern the nature of the mechanism of alkylation of [Tm^{Ph}]ZnSCH$_2$C(O)N(H)Ph. However, the situation is such that the kinetics studies are unable to distinguish between associative and dissociative reaction mechanisms. For example, although the pseudo-first-order rate constant (k_{obs}) for the reaction of [Tm^{Ph}]ZnSCH$_2$C(O)N(H)Ph with excess MeI (see Supporting Information) is dependent on the concentration of MeI and is in accord with a rate law of the type $d[ZnSR]/dt = -k[ZnSR][MeI]$ ($k = 2.34(13) \times 10^{-4}$ M^{-1} s^{-1} at 0 °C), this observation does not provide definitive evidence that the mechanism is associative. Specifically, a dissociative reaction can also exhibit second-order kinetics if recoordination of RS$^-$ to the zinc center competes with alkylation by MeI. Only if saturation kinetics is observed (i.e., the rate becomes independent of MeI concentration and the first step is rate determining) can one definitively conclude that the mechanism is dissociative. Thus, while the kinetics are consistent with an associative mechanism, they do not preclude a dissociative mechanism.

In addition to the kinetics, the activation parameters derived from the temperature dependence of the second order rate constant (see Supporting Information), namely, $\Delta H^{\ddagger} = 14.1(1.0)$ kcal mol^{-1} and $\Delta S^{\ddagger} = -23.1(3.5)$ eu, do not definitively distinguish between associative and dissociative mechanisms. Thus, although the negative value of $\Delta S^{\ddagger}$ is consistent with an associative mechanism, it is also consistent with a dissociative mechanism if electrostriction resulting from solvation of the cation and anion causes a significant ordering of the solvent.[48] As a consequence, the negative value of $\Delta S^{\ddagger}$ does not unambiguously establish the nature of the mechanism. It is, nevertheless, pertinent to note that comparable values have been reported for thiolate alkylation in other systems. For example, methylation of [Ph(pz$^{Bu^t}$)Bt$^{Bu^t}$]ZnSPh by MeI is characterized by a value of $\Delta S^{\ddagger} = -21.5(2.7)$ eu,[32] while methylation of HC(pz^{Me_2})$_2$(C$_6$H$_2$Bu^{t}MeO)]ZnCH$_2$Bz is characterized by a value of $\Delta S^{\ddagger} = -35$ eu.[43,49,50] In view of the fact that the kinetics studies do not provide a definitive answer with respect to the mechanism of thiolate alkylation, the mechanism has also been probed by evaluating kinetic deuterium isotope effects, as described below.

Influence of the Intramolecular NH···S Hydrogen Bond on Thiolate Alkylation as Probed by Kinetic Deuterium Isotope Effects. Since [Tm^{Ph}]ZnSCH$_2$C(O)N(H)Ph exhibits an intramolecular NH···S hydrogen bond, an important question is concerned with how this interaction influences the susceptibility of the thiolate ligand towards alkylation. In this regard, an indication that N—H···S hydrogen bonding interactions may reduce the nucleophilicity of a thiolate ligand is provided by the observation that hydrogen bonded LZnS[C$_6$H$_4$-*o*-NHC(O)R] derivatives exhibit a lower reactivity than the corresponding phenylthiolate complex LZnSPh towards alkyl halides.[31,32]

It is well-established that kinetic deuterium isotope effects provide valuable information concerned with the mechanism of reactions,[51] and for this reason, it is important to determine how isotopic substitution influences the N—**H***···S (H* = H, D) hydrogen bonding interaction and the subsequent impact on the rate of alkylation of a thiolate ligand. To address this issue, we have determined the kinetic isotope effect (KIE) for alkylation of [Tm^{Ph}]ZnSCH$_2$C(O)N(**H***)Ph by MeI. Interestingly, the alkylation of [Tm^{Ph}]ZnSCH$_2$C(O)N(**H***)Ph is characterized by a small normal (i.e., $k_H/k_D > 1$) value of $k_H/k_D = 1.16(1)$ at 0 °C, in marked contrast to the substantial inverse (i.e., $k_H/k_D < 1$) value of 0.33 reported by Riordan for alkylation of [Ph(pz^{But})Bt^{But}]ZnS[C$_6$H$_4$-*o*-N**H***C(O)Bu^t] by PhCH$_2$Br.[32]

In order to place these differing KIEs in context, it is necessary to understand how changes in N—**H***···S hydrogen bonding interactions influence kinetic and equilibrium isotope effects for a variety of elementary transformations, especially because it is recognized that there are classes of reactions that exhibit both normal and inverse KIEs depending on the specific system. The occurrence of both normal and inverse KIEs for a particular class of reaction is normally a consequence of the reaction being composed of a multistep sequence. For multistep reactions, the observed KIE is a composite of the KIEs of all steps (including their microscopic reverse) up to and including the rate determining step; a change in the rate determining step may thus have a pronounced effect on the overall KIE. Consider, for example, the KIE for reductive elimination of RH and RD from transition metal alkyl-hydride compounds, [M(R)H] and [M(R)D], which has been shown to occur with both normal and inverse KIEs.[52] The reductive elimination of methane from an alkyl-hydride compound [M(R)H] is recognized to be a two-step process involving (i) reductive coupling to form a σ-complex intermediate [M(σ-RH)] followed by (ii) dissociation of RH. If the first step is rate determining, the KIE corresponds specifically to reductive coupling step and is normal because the M—H and M—D bonds start to break on going to the transition state. However, if the second step is rate determining, the observed KIE is a composite that includes the equilibrium isotope effect (EIE) for formation of the σ-complex intermediate [M(σ-RH)]. Unlike single-step primary kinetic deuterium isotope effects that are customarily normal, equilibrium deuterium isotope effects may be either normal or inverse and depend critically upon zero point energy differences and vibrational excitation components.[53] The EIE for the interconversion of [M(R)X] and [M(σ-RX)] (X = H, D) is inverse because the zero point energy of the system is lower if deuterium is attached to carbon;[54] thus, an overall inverse KIE for reductive elimination of methane may be observed if the second step (i.e., dissociation of methane) is rate determining.[52] In light of the above discussion, it is evident that any interpretation of the observed kinetic deuterium isotope effect for alkylation of

(48) Atwood, J. A. *Inorganic and Organometallic Reaction Mechanisms*, 2nd ed.; VCH: New York, 1997.
(49) The value reported, $\Delta S^{\ddagger} = -35$ kcal mol^{-1} K^{-1}, is a typographical error and should be -35 cal mol^{-1} K^{-1} (Carrano, C. J., personal communication).
(50) For a compilation of $\Delta S°$ values, see Minas da Piedade, M. E.; Martinho Simões, J. A. *J. Organomet. Chem.* **1996**, *518*, 167−180.
(51) (a) Bullock, R. M.; Bender, B. R. Isotope Methods in Homogeneous Catalysis. In *Encyclopedia of Catalysis*; Horváth, I. T., Ed.; 2002. (b) Jones, W. D. *Acc. Chem. Res.* **2003**, *36*, 140−146. (c) Matsson, O.; Westaway, K. C. *Adv. Phys. Org. Chem.* **1998**, *31*, 143−248. (d) Rosenberg, E. *Polyhedron* **1989**, *8*, 383−405. (e) Anderson, V. E. *Curr. Opin. Struct. Biol.* **1992**, *2*, 757−764. (f) Kohen, A. *Prog. React. Kinet. Mech.* **2003**, *28*, 119−156.
(52) See, for example (a) Churchill, D. G.; Janak, K. E.; Wittenberg, J. S.; Parkin, G. *J. Am. Chem. Soc.* **2003**, *125*, 1403−1420. (b) Janak, K. E.; Churchill, D. G.; Parkin, G. *Activation Funct. C−H Bonds, ACS Symp. Ser.* **2004**, *885*, 86−104.
(53) See, for example (a) Janak, K. E.; Parkin, G. *J. Am. Chem. Soc.* **2003**, *125*, 6889−6891. (b) Janak, K. E.; Parkin, G. *Organometallics* **2003**, *22*, 4378−4380. (c) Janak, K. E.; Parkin, G. *J. Am. Chem. Soc.* **2003**, *125*, 13219−13224. (d) Janak, K. E.; Shin, J. H.; Parkin, G. *J. Am. Chem. Soc.* **2004**, *126*, 13054−13070.
(54) Janak, K. E.; Churchill, D. G.; Parkin, G. *Chem. Commun.* **2003**, 22−23.

Scheme 3

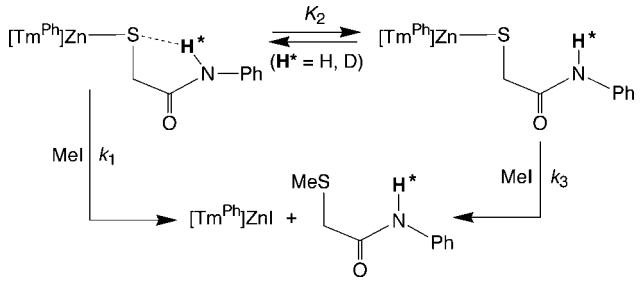

[Tm^{Ph}]ZnSCH$_2$C(O)N(**H**)Ph and [Tm^{Ph}]ZnSCH$_2$C(O)N(**D**)Ph by MeI requires knowledge of the isotope effects for the individual steps of the mechanism, as addressed below.

Calculation of Kinetic and Equilibrium Deuterium Isotope Effects Relevant to Thiolate Alkylation. To establish whether a given mechanism is consistent with an observed KIE, it is necessary to have knowledge of the isotope effects for each individual step up to and including the rate determining step. Experimental determination of kinetic and equilibrium isotope effects of individual steps in a multistep reaction is, however, a nontrivial task. It is, therefore, significant that calculations have been shown to be of considerable use in providing a detailed understanding of isotope effects in a variety of systems.[55] For this reason, we have used DFT calculations to compute isotope effects in an effort to determine which mechanism is most consistent with the observed KIE for alkylation of [Tm^{Ph}]ZnSCH$_2$C(O)N(**H***)Ph by MeI.

Kinetic and equilibrium isotope effects are commonly determined by using the expression k_H/k_D (or K_H/K_D) = SYM·MMI·EXC·ZPE, where SYM is the symmetry factor, MMI is the mass-moment of inertia term, EXC is the excitation term, and ZPE is the zero point energy term.[56] The SYM term is determined by the symmetry number ratio of the species involved; the MMI term is determined by their structures (i.e., their masses and moments of inertia); and the EXC and ZPE terms are determined by their vibrational frequencies. Since the determination of frequencies is highly computationally intensive, calculations were performed on a computationally simpler system, namely, [Tm^{H}]ZnSCH$_2$C(O)N(**H***)Ph and its derivatives, in which the phenyl substituents of the [Tm^{Ph}] ligand are replaced by hydrogen.

Associative Mechanisms: Isotope effects for (a) the Interconversion of the Hydrogen Bonded and Non-Hydrogen Bonded Isomers of [Tm^{H}]ZnSCH$_2$C(O)N(H*)Ph and (b) Methylation of [Tm^{H}]ZnSCH$_2$C(O)N(H*)Ph by MeI. Two of the simplest possibilities that involve an associative mechanism are illustrated in Scheme 3 and involve (i) direct reaction of MeI with the experimentally observed N—H···S hydrogen bonded structure of [Tm^{Ph}]ZnSCH$_2$C(O)N(H)Ph (k_1) and (ii) rapid isomerization of the N—H···S hydrogen bonded structure

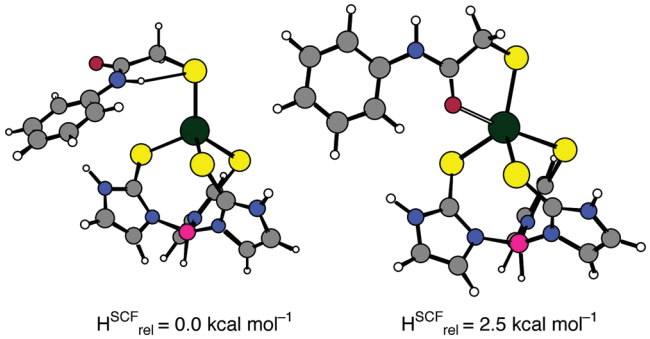

Figure 4. Geometry optimized structures of [Tm^{H}]ZnSCH$_2$C(O)N(H)Ph with and without N—H···S hydrogen bonds.

Scheme 4

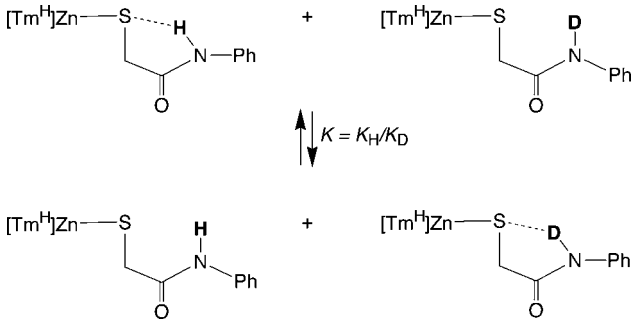

of [Tm^{Ph}]ZnSCH$_2$C(O)N(H)Ph to a non-hydrogen bonded structure ($K_2 = k_2/k_{-2}$) followed by a rate determining reaction with MeI (k_3). The latter mechanism is particularly relevant since it has been postulated that N—H···S hydrogen bonding interactions temper the susceptibility of a thiolate ligand towards alkylation.[10,11] Whereas the observed KIE for the former mechanism would simply correspond to a secondary KIE for a single step (k_{1H}/k_{1D}), that for the latter reaction is a composite that includes the EIE for the interconversion of hydrogen bonded and non-hydrogen bonded isomers (K_{2H}/K_{2D}). Since the N**H*** group does not participate in the second step of the reaction, the KIE for this step would be expected to be minimal (i.e., $k_{3H}/k_{3D} \approx 1$); as a consequence, the KIE for alkylation would be expected to correspond closely to the EIE for the interconversion of hydrogen bonded and non-hydrogen bonded isomers. The EIE for interconversion between the hydrogen bonded and non-hydrogen bonded forms has, therefore, been determined by DFT calculations on the isomers of [Tm^{H}]-ZnSCH$_2$C(O)N(H)Ph.

The geometry optimized structure of [Tm^{H}]ZnSCH$_2$C(O)N-(H)Ph is illustrated in Figure 4, and key features of the N—H···S hydrogen bonding interaction correspond closely to those of the full molecule [Tm^{Ph}]ZnSCH$_2$C(O)N(H)Ph. Thus, the NH···S and N···S separations of 2.39 and 3.03 Å, respectively, for the smaller analogue [Tm^{H}]ZnSCH$_2$C(O)N(H)Ph compare favorably with the corresponding values of 2.36 and 3.02 Å for the full molecule [Tm^{Ph}]ZnSCH$_2$C(O)N(H)Ph. It is also noteworthy that the hydrogen bonded structure of [Tm^{H}]ZnSCH$_2$C(O)N(H)Ph is 2.5 kcal mol^{-1} more stable than the non-hydrogen bonded form (Figure 4), which possesses a modified structure in which the amide oxygen exhibits a weak interaction with the zinc (d_{Zn-O} = 2.30 Å).

Computation of all vibrational frequencies for the hydrogen bonded and non-hydrogen bonded forms of [Tm^{H}]ZnSCH$_2$C-(O)N(**H***)Ph (see Supporting Information) allows the EIE for

(55) See, for example (a) Slaughter, L. M.; Wolczanski, P. T.; Klinckman, T. R.; Cundari, T. R. *J. Am. Chem. Soc.* **2000**, *122*, 7953−7975. (b) Bender, B. R. *J. Am. Chem. Soc.* **1995**, *117*, 11239−11246. (c) Abu-Hasanayn, F.; Krogh-Jespersen, K.; Goldman, A. S. *J. Am. Chem. Soc.* **1993**, *115*, 8019−8023. (d) Bender, B. R.; Kubas, G. J.; Jones, L. H.; Swanson, B. I.; Eckert, J.; Capps, K. B.; Hoff, C. D. *J. Am. Chem. Soc.* **1997**, *119*, 9179−9190. (e) Refs 53 and 54.

(56) (a) Wolfsberg, M.; Stern, M. J. *Pure Appl. Chem.* **1964**, *8*, 225−242. (b) Melander, L.; Saunders, W. H., Jr. *Reaction Rates of Isotopic Molecules*; Wiley-Interscience: New York, 1980. (c) Carpenter, B. K. *Determination of Organic Reaction Mechanisms*; Wiley-Interscience: New York, 1984. (d) Ishida, T. *J. Nucl. Sci. Technol.* **2002**, *39*, 407−412. (e) Bigeleisen, J.; Mayer, M. G. *J. Chem. Phys.* **1947**, *15*, 261−267.

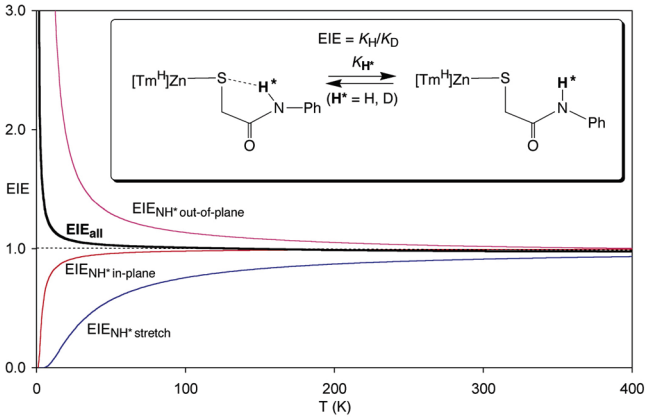

Figure 5. Temperature dependence of the EIE for the interconversion of the hydrogen bonded and non-hydrogen bonded isomers [Tm^H]ZnSCH$_2$C(O)N(**H***)Ph.

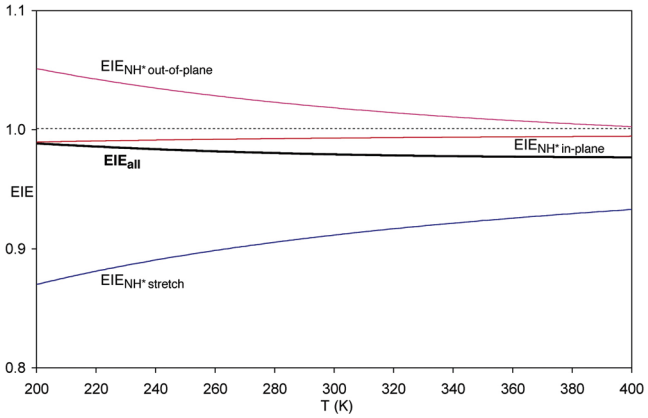

Figure 6. Temperature dependence of the EIE for the interconversion of the hydrogen bonded and non-hydrogen bonded isomers [Tm^H]ZnSCH$_2$C(O)N(**H***)Ph, emphasizing how the negligible isotope effect at ambient temperature is a result of opposing contributions from the N−H* stretches and N−H out-of-plane bends.

the interconversion of the hydrogen bonded and non-hydrogen bonded isomers (Scheme 4) to be determined. As illustrated by the temperature dependence shown in Figures 5 and 6, the EIE is normal at low temperatures but approaches unity at higher temperatures. A detailed examination of the temperature profile indicates that the EIE actually becomes slightly inverse (with a minimum value of 0.977 at 420 K) before returning to unity at high temperatures. Examination of Figure 6 indicates that the EIE is relatively insensitive to temperature over the range of 200−400 K and is calculated to be 0.98 at 0 °C, the temperature at which the KIE was experimentally measured.

Although the EIE is determined by all molecular vibrations, the three most sensitive to isotopic substitution are those associated with the N−H* bond, namely, a N−H stretch, an in-plane bend, and out-of-plane bend.[57] Examination of these three components demonstrates that the negligible value for the EIE at 0 °C is a result of competing effects arising from the fact that the hydrogen bonding interaction results in opposing shifts in the frequencies of these vibrations.[58] Thus, as summarized in Table 2, while the N−H* stretch in the hydrogen bonded isomer is lower in energy than that in the non-hydrogen bonded isomer, the converse is true for the out-of-plane bend; the in-plane bend, however, is virtually insensitive to the hydrogen bonding interaction.

The individual components of these vibrations to the EIE are illustrated in Figures 5 and 6, which demonstrate that while the contribution of the N−H and N−D stretches favors an inverse EIE (with deuterium preferring to reside in the non-hydrogen bonded isomer), the contribution from the out-of-plane bend favors a normal EIE (with deuterium preferring to reside in the hydrogen bonded isomer). As a result of these opposing effects, the EIE for interconversion of the hydrogen bonded and non-hydrogen bonded isomers is calculated to be negligible at ambient temperature.

With respect to the KIE for methylation of [Tm^H]ZnSCH$_2$C(O)N(**H***)Ph by MeI, we have calculated the isotope effects for associative pathways that include a (i) rate determining S$_N$2 like displacement of iodide by the coordinated zinc thiolate ligand and (ii) a four-centered transition state that features Zn···I bond formation concomitant with Me···SR bond formation (Scheme 2). Since the KIE for a product-like transition state approaches that for an EIE,[59] an approximation that is especially valid for secondary KIEs, the equilibrium isotope effect for the first step of the stepwise associative mechanism (Scheme 2, mechanism i) has been determined. For this purpose, the molecular structure and vibrational frequencies of the methylated cation {[Tm^H]Zn[S(Me)CH$_2$C(O)N(**H***)Ph]}$^+$ (Figure 7) have been determined by DFT calculations, from which the EIE for the methylation of [Tm^H]ZnSCH$_2$C(O)N(**H***)Ph (Scheme 5) has been obtained as a function of temperature (Figure 8). Notably, the EIE is calculated to be inverse at all temperatures, with a value of 0.94 at 0 °C. As with the EIE for the interconversion of the hydrogen bonded and non-hydrogen bonded isomers of [Tm^H]ZnSCH$_2$C(O)N(**H***)Ph, the small isotope effect is a consequence of opposing contributions from the N−H* stretch and out-of-plane bend that, respectively, favor an inverse and normal isotope effect.

The KIE for a single step alkylation mechanism (Scheme 2, mechanism ii) has been determined by performing a geometry optimization of the four-centered associative transition state for metathesis of the Zn−S and C−I bonds as illustrated in Figure 7. The structure of the {[Tm^H]ZnSCH$_2$C(O)N(H)Ph}···MeI}‡ transition state is based on a trigonal bipyramidal geometry at zinc with iodine in an axial site and is characterized by the following bond lengths: Zn−S (2.430 Å), S−C (2.642 Å), C−I

(57) While these three vibrations are highly isotopically sensitive, with a vibrational product $\pi(\nu_H/\nu_D)$ that is very similar to that predicted using the Teller−Redlich product rule, it is important to note that they are not the only components of the isotope effect and that the other vibrations play a role due to coupling. For example, the amide II and III bands are, respectively, the out-of-phase and in-phase combinations of the NH in-plane bend and CN stretch.[a−c] The limiting isotope effect at 0 K is determined by the ZPE term, and small variations in vibrational frequencies are sufficient to cause the neglible isotope effect at ambient temperature to become either strongly normal or inverse at low temperature. (a) Watson, T. M.; Hirst, J. D. *J. Phys. Chem. A* **2002**, *106*, 7858−7867. (b) Arjunan, V.; Mohan, S.; Subramanian, S.; Thimme Gowda, B. *Spectrochim. Acta A* **2004**, *60*, 1141−1159. (c) Herrebout, W. A.; Clou, K.; Desseyn, H. O. *J. Phys. Chem. A* **2001**, *105*, 4865−4881.

(58) It is well-known that different vibrations may provide comparable and opposing contributions that minimize the magnitude of secondary isotope effects. See, for example (a) Glad, S. S.; Jensen, F. *J. Am. Chem. Soc.* **1997**, *119*, 227−232. (b) Ruggiero, G. D.; Williams, I. H.; Roca, M.; Moliner, V.; Tuñón, I. *J. Am. Chem. Soc.* **2004**, *126*, 8634−8635. (c) Moliner, V.; Williams, I. H. *J. Am. Chem. Soc.* **2000**, *122*, 10895−10902. (d) Hu, W.-P.; Truhlar, D. G. *J. Am. Chem. Soc.* **1995**, *117*, 10726−10734. (e) Barnes, J. A.; Williams, I. H. *J. Chem. Soc., Chem. Commun.* **1993**, 1286−1287. (f) Poirier, R. A.; Wang, Y.; Westaway, K. C. *J. Am. Chem. Soc.* **1994**, *116*, 2526−2533. (g) Lee, I. *Chem. Soc. Rev.* **1995**, 223−229. (h) Hasanayn, F.; Streitwieser, A.; Al-Rifai, R. *J. Am. Chem. Soc.* **2005**, *127*, 2249−2255. (i) Ref 51c.

(59) Saunders, W. H., Jr. *Tech. Chem.* **1986**, *6*, Part 1, 565−611.

Table 2. Principal Isotopically Sensitive Vibrations[a]

	H-bonded [Tm^{H}]ZnSC H_2C(O)N(**H***)Ph	non-H-bonded [Tm^{H}]ZnSC H_2C(O)N(**H***)Ph	{[Tm^{H}]ZnS(Me)-CH_2C(O)N(**H***)Ph}$^+$	{[Tm^{H}]ZnSCH_2C-(O)N(**H***)Ph}···MeI}‡	[SCH_2C-(O)N(**H***)Ph]$^-$	{PhN(**H***)C-(O)CH_2S···MeI}‡
ν(N−H*$_{stretch}$)/cm^{-1}	3464.5 (2547.4)	3602.6 (2647.0)	3591.3 (2631.9)	3508.7 (2579.6)	3067.6 (2255.5)	3267.2 (2398.4)
ν(N−H*$_{in-plane}$)/cm^{-1}	1572.3 (1026.1)	1571.5 (1022.5)	1573.3 (1039.1)	1568.5 (1024.0)	1579.9 (1025.4)	1580.5 (1025.4)
ν(N−H*$_{out-of-plane}$)/cm^{-1}	722.7 (540.3)	611.3 (446.5)	570.5 (431.2)	665.0 (491.9)	823.1 (610.3)	792.8 (577.7)

[a] Values listed in parentheses for **H*** = D.

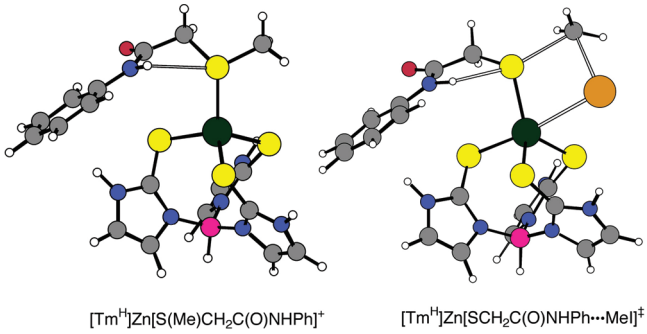

Figure 7. Geometry optimized structures of {[Tm^{H}]Zn[S(Me)CH_2C(O)N-(H)Ph]}$^+$ and {[Tm^{H}]ZnSCH_2C(O)N(H)Ph}···MeI}‡.

Scheme 5

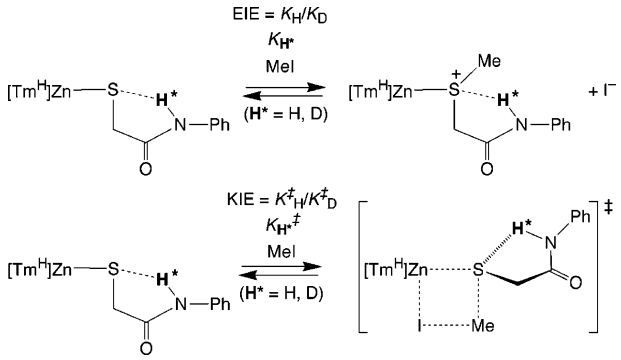

(2.971 Å), and Zn−I (3.406 Å).[60] As would be expected, the Zn−S bond length is intermediate between that in [Tm^{H}]-ZnSCH_2C(O)N(H)Ph (2.354 Å) and {[Tm^{H}]Zn[S(Me)CH_2C-(O)N(H)Ph]}$^+$ (2.592 Å). The N−H···S hydrogen bonding interaction in the transition state is not, however, significantly perturbed from that in [Tm^{H}]ZnSCH_2C(O)N(H)Ph (Table 3). As a consequence of the similar hydrogen bonding interaction and the fact that the N−H* stretch and out-of-plane bend (Table 2) have opposing contributions, the KIE as defined in Scheme 5 is negligible, with a value of 1.00 at 0 °C (Figure 9).

Dissociative Mechanism: Equilibrium Isotope Effect for Thiolate Dissociation from [Tm^{H}]ZnSCH_2C(O)N(H*)Ph and Kinetic Isotope Effect for S_N2 Displacement of I$^-$ by [PhN(H*)C(O)CH_2S]$^-$. The observed second-order kinetics are also consistent with a dissociative mechanism in which the second step is rate determining (Scheme 6). Therefore, the EIE for the dissociation of [PhN(**H***)C(O)CH_2S]$^-$ from [Tm^{H}]-ZnSCH_2C(O)N(**H***)Ph (Scheme 6) plays an important role in determining the overall KIE for this mechanism. As illustrated in Figure 10, the EIE is normal at all temperatures, with a value of 1.21 at 0 °C. The EIE is dominated by the component due to the N−H* stretch and is normal because the N−H* stretch in [PhN(**H***)C(O)CH_2S]$^-$ (Figure 11) is significantly lower in

(60) These structural parameters are very different to those calculated for [$(H_3N)_3$-Zn(SMe)···MeI]‡ at the PM3 level using MOPAC: Zn−S (2.53 Å), S−C (2.34 Å), C−I (2.55 Å), and Zn−I (2.59 Å). See ref 43.

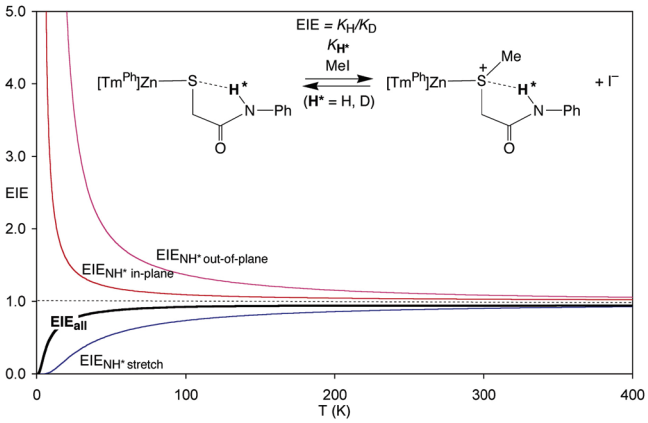

Figure 8. Temperature dependence of the EIE for the methylation of [Tm^{H}]ZnSCH_2C(O)N(**H***)Ph to give {[Tm^{H}]Zn[S(Me)CH_2C(O)N(**H***)-Ph]}$^+$.

energy than that in [Tm^{H}]ZnSCH_2C(O)N(**H***)Ph (Table 2), a consequence of the fact that the hydrogen bonding interaction is stronger in anionic [PhN(**H***)C(O)CH_2S]$^-$ due to the negative charge on sulfur, which makes it a better hydrogen bond acceptor. For example, the N−H bond length increases from 1.01 Å in [Tm^{H}]ZnSCH_2C(O)N(H)Ph to 1.04 Å in [PhN(H)C-(O)CH_2S]$^-$, while the S···H distance decreases from 2.39 to 2.16 Å (Table 3). However, while the increased hydrogen bonding interaction in [PhN(**H***)C(O)CH_2S]$^-$ results in a shift of the N−H* stretch to lower energy, it also causes the out-of-plane bend to shift to higher energy, which therefore minimizes the isotope effect.

The second step of the dissociative mechanism involves S_N2 displacement of I$^-$ by [PhN(**H***)C(O)CH_2S]$^-$ (Scheme 6), the transition state of which is illustrated in Figure 11. The KIE for this reaction is calculated to be inverse at all temperatures, with a value of 0.89 at 0 °C (Figure 12). The isotope effect is dominated by the component due to the N−H* stretch and is inverse because ν(N−H*) for the transition state [PhN(**H***)C(O)CH_2S···Me···I]$^{‡-}$ is significantly higher in energy than that for [PhN(**H***)C(O)CH_2S]$^-$ (Table 2). Since the inverse KIE for the second step opposes the normal EIE for the first step, the overall isotope effect is reduced from a value of 1.21 for the EIE to a value 1.08 at 0 °C.[61]

Comparison of Kinetic and Equilibrium Isotope Effects as a Function of the Magnitude of the N−H*···S Hydrogen Bonding Interaction. The kinetic and equilibrium isotope effects for the various reactions studied are summarized in Table 4, while details pertaining to the N−H···S hydrogen bonding interactions are summarized in Table 3. Although the isotope effects are large (normal or inverse) at low temperatures, they

(61) This value for the overall isotope effect assumes that the barrier for the second step is significantly greater than that for the first step (i.e., the condition required to observe second-order kinetics). As the barrier for the second step approaches that for the first step, the overall kinetic isotope effect approaches that for the first step.

Table 3. Summary of N—H···S Hydrogen Bonding Interactions in Species Containing [SCH$_2$C(O)N(H)Ph]

	H-bonded [Tm^{H}]ZnSCH$_2$C(O)N(H)Ph	non-H-bonded [Tm^{H}]ZnSCH$_2$C(O)N(H)Ph	{[Tm^{H}]ZnS(Me)-CH$_2$C(O)N(H)Ph}$^+$	{[Tm^{H}]ZnSCH$_2$C-(O)N(H)Ph}···MeI}‡	[SCH$_2$C-(O)N(H)Ph]$^-$	[PhN(H)C-(O)CH$_2$S···MeI]$^{-‡}$
d_{N-H}/Å	1.019	1.012	1.013	1.017	1.043	1.031
$d_{S\cdots H}$/Å	2.387		2.700	2.435	2.164	2.244
$d_{N\cdots S}$/Å	3.034		3.070	3.049	2.933	2.970

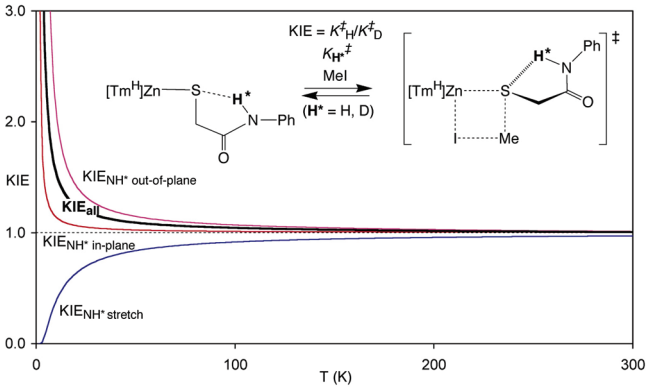

Figure 9. Temperature dependence of the KIE for the methylation of [Tm^{H}]ZnSCH$_2$C(O)N(**H***)Ph via a four-centered {[Tm^{H}]ZnSCH$_2$C(O)N-(**H***)Ph}···MeI}‡ transition state.

Scheme 6

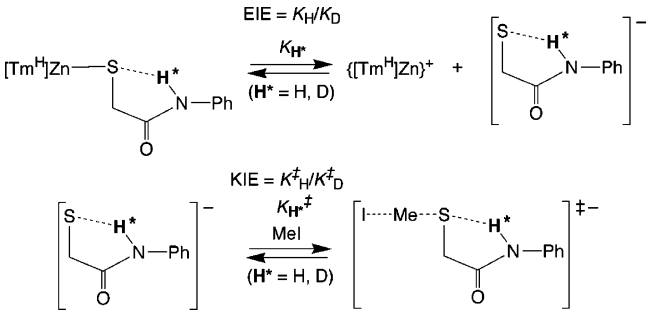

are small at ambient temperatures, irrespective of whether the N—H···S hydrogen bonding interaction becomes stronger or weaker in the product. As noted above, the origin of this insensitivity of the isotope effect is the fact that the N—H stretch and out-of-plane bend are influenced oppositely as the strength of the N—H···S hydrogen bonding increases. A simple gauge of the magnitude of the hydrogen bonding interaction is provided by the N—H and N···S distances (Table 3), and the two extremes are represented by the non-hydrogen bonded form of [Tm^{H}]ZnSCH$_2$C(O)N(H)Ph and the anion [PhN(H)C(O)CH$_2$S]$^-$. The extent of the hydrogen bonding interaction is a function of the ability of the sulfur to serve as a hydrogen bond acceptor, which clearly correlates with the negative charge on sulfur. Thus, relative to the hydrogen bonded form of [Tm^{H}]ZnSCH$_2$C(O)N-(H)Ph, the anion [PhN(H)C(O)CH$_2$S]$^-$ exhibits a stronger N—H···S hydrogen bonding interaction, while the cation {[Tm^{H}]Zn[S(Me)CH$_2$C(O)N(H)Ph]}$^+$ exhibits a weaker interaction.

The influence of the hydrogen bonding interaction (as judged by the N—H bond distance) on the frequencies of the N—H stretch, in-plane bend, and out-of-plane bend is illustrated in Figure 13. These correlations clearly indicate that the frequency of the N—H stretch decreases as the N—H···S hydrogen bonding interaction increases, while the frequency of the N—H out-of-plane bend increases; the N—H in-plane bend, however, is relatively insensitive to the hydrogen bonding interaction.

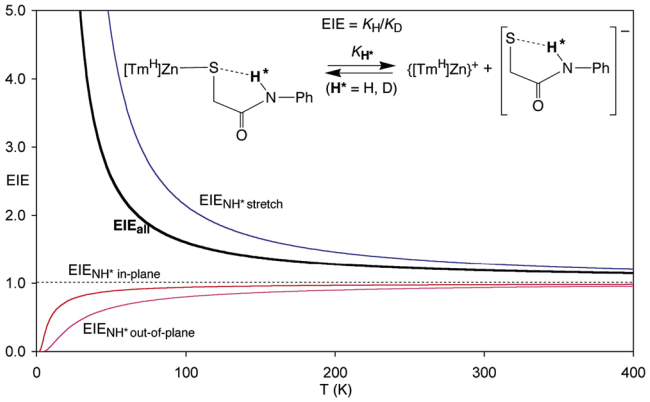

Figure 10. Temperature dependence of the EIE for dissociation of [PhN(**H***)C(O)CH$_2$S]$^-$ from [Tm^{H}]ZnSCH$_2$C(O)N(**H***)Ph.

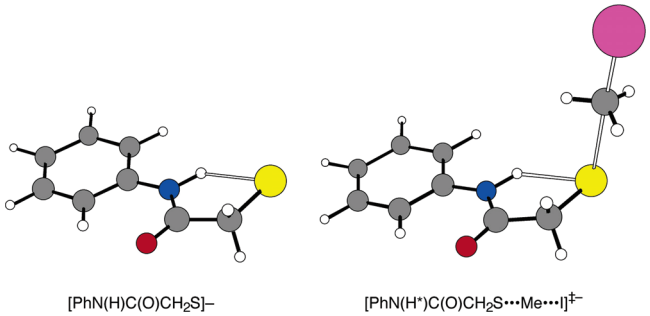

Figure 11. Geometry optimized structures of [PhN(H)C(O)CH$_2$S]$^-$ and the transition state [PhN(**H***)C(O)CH$_2$S···Me···I]$^{‡-}$.

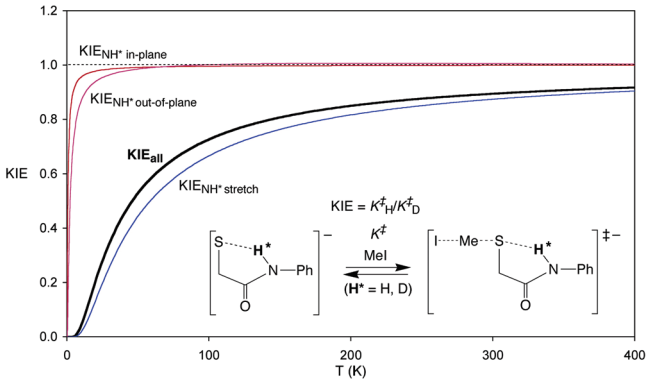

Figure 12. Temperature dependence of the KIE for the reaction of [PhN(**H***)C(O)CH$_2$S]$^-$ with MeI.

The zero point energy (ZPE) component of the isotope effect is determined by the variation in vibrational frequencies, such that a decrease in frequency of a particular vibrational mode gives rise to a normal ZPE component of the isotope effect, whereas an increase in energy of a particular vibrational mode gives rise to an inverse ZPE component.[62] Since the frequencies

(62) For example, if one considers for simplicity a single isotopically sensitive vibration in the reactant and product, and if it is assumed that the ratio ν_H/ν_D is a constant (x) for both species involved in the equilibrium, then $K_H/K_D = \exp[\Delta\nu_H\{1 - (1/x)\}h/2k_BT]$, where $\Delta\nu_H$ is defined as $\nu_{H(react)} - \nu_{H(prod)}$. For $x > 1$, $K_H/K_D < 1$ if $\Delta\nu_H < 0$ and $K_H/K_D > 1$ if $\Delta\nu_H > 0$.

Table 4. Summary of Isotope Effects at 0 °C

reaction	isotope effect
$[Tm^{Ph}]ZnSCH_2C(O)N(\mathbf{H^*})Ph + MeI \xrightarrow{k_{H^*}} [Tm^{Ph}]ZnI + PhN(\mathbf{H^*})C(O)CH_2SMe$	$k_H/k_D = 1.16(1)^a$
H-bonded $[Tm^H]ZnSCH_2C(O)N(\mathbf{H^*})Ph \overset{K_{H^*}}{\rightleftharpoons}$ non-H-bonded $[Tm^H]ZnSCH_2C(O)N(\mathbf{H^*})Ph$	$K_H/K_D = 0.98^b$
$[Tm^H]ZnSCH_2C(O)N(\mathbf{H^*})Ph + MeI \overset{K_{H^*}}{\rightleftharpoons} \{[Tm^H]ZnS(Me)CH_2C(O)N(\mathbf{H^*})Ph\}^+ + I^-$	$K_H/K_D = 0.94^b$
$[Tm^H]ZnSCH_2C(O)N(\mathbf{H^*})Ph + MeI \xrightarrow{k_{H^*}} \{[Tm^H]ZnSCH_2C(O)N(\mathbf{H^*})Ph\}\cdots MeI^{\ddagger\,c}$	$k_H/k_D = 1.00^b$
$[Tm^H]ZnSCH_2C(O)N(\mathbf{H^*})Ph \overset{K_{H^*}}{\rightleftharpoons} \{[Tm^H]Zn^+ + PhN(\mathbf{H^*})C(O)CH_2S^-$	$K_H/K_D = 1.21^b$
$PhN(\mathbf{H^*})C(O)CH_2S^- + MeI \xrightarrow{k_{H^*}} [PhN(H)C(O)CH_2S\cdots Me\cdots I]^{-\,\ddagger\,d}$	$k_H/k_D = 0.89^b$

[a] Experimental value. [b] Calculated value. [c] Four-center transition state. [d] S_N2 transition state.

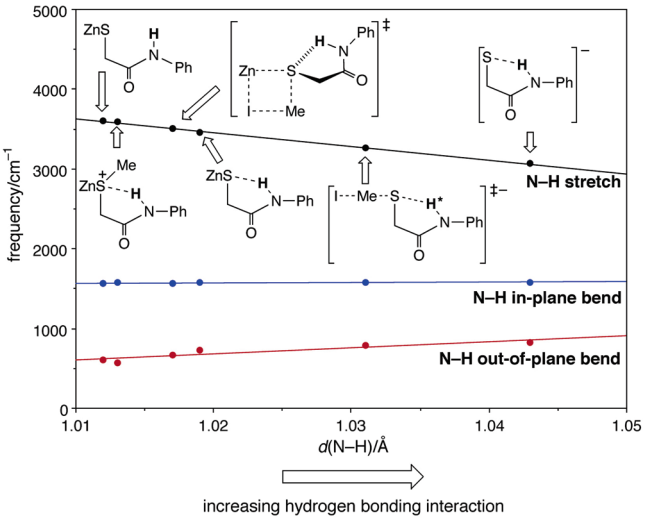

Figure 13. Correlation of N−H stretch, in-plane bend, and out-of-plane bend with d_{N-H} as an indicator of the strength of the hydrogen bonding interaction in various {PhN(H)C(O)CH$_2$S} derivatives.

of the N−H stretch and N−H out-of-plane bends are influenced oppositely by the N−H···S hydrogen bonding interaction, the components of these vibrations to the isotope effect mitigate each other, with the result that all of the isotope effects are close to unity at ambient temperature. However, despite the fact that the calculated isotope effects are small, it is evident that the only mechanism that gives rise to a normal KIE is one involving a dissociative step (Figure 10). On this basis, the experimentally determined KIE of 1.16(1), albeit close to unity, is more in accord with a dissociative rather than associative mechanism.

While it is clear that a mechanism involving initial dissociation of the zinc−thiolate ligand is more consistent with the observed normal KIE than is a mechanism involving direct alkylation of the zinc−thiolate ligand, it is important to note that it is also possible for more complex mechanisms to be characterized by a normal KIE. Specifically, a normal KIE is merely a consequence of a mechanism in which the N−H···S hydrogen bonding interaction increases; thus, any mechanism that results in such a change could, in principle, be associated with a normal KIE. An increase in the N−H···S hydrogen bonding interaction occurs when a step results in an increase in the negative charge on sulfur; thus, any step that satisfies this criterion should favor a normal KIE. For example, it is possible that MeI could associatively displace thiolate to give $\{[Tm^{Ph}]Zn(IMe)\}^+$ and $[PhN(H)C(O)CH_2S]^-$ and that this step would be characterized by a normal isotope effect because thiolate dissociation is an important component. The essential feature, therefore, is that a normal KIE requires substantial cleavage of the zinc−thiolate bond prior to sulfur alkylation. Correspondingly, it is unlikely that a normal KIE could result from any mechanism that involves direct alkylation of a zinc−thiolate ligand because the hydrogen bonding interaction is necessarily weakened and an isotope effect of $k_H/k_D \leq 1$ is predicted. Issues that remain to be addressed by comparison to other derivatives are whether the proposed dissociative mechanism for $[Tm^R]ZnSCH_2C(O)N(H)Ph$ is a consequence of (i) the electron rich [S_3] donor ligand, which facilitates thiolate dissociation or (ii) hydrogen bond stabilization of the $[PhN(H)C(O)CH_2S]^-$ anion.

Conclusions

In summary, $[Tm^{Ph}]ZnSCH_2C(O)N(H)Ph$ is a tetrahedral zinc−thiolate complex with a [S_4Zn] core that features an intramolecular N−H···S hydrogen bond. $[Tm^{Ph}]ZnSCH_2C(O)N(H)Ph$ not only serves as a structural model for the Ada DNA repair protein but also mimics its function with respect to thiolate alkylation via the reaction with MeI to yield $PhN(H)C(O)CH_2SMe$ and $[Tm^{Ph}]ZnI$. The mechanism of the thiolate alkylation has been investigated by kinetics studies which indicate that the reaction is characterized by second-order kinetics that are consistent with either (i) an associative mechanism or (ii) a stepwise dissociative mechanism in which the thiolate alkylation is rate determining. Although the kinetics studies are incapable of distinguishing between these possibilities, kinetic isotope measurements on the isotopologues $[Tm^{Ph}]ZnSCH_2C(O)N(\mathbf{H^*})Ph$ ($\mathbf{H^*}$ = H, D) are more in accord with a dissociative mechanism. In particular, the KIE for the reaction of $[Tm^{Ph}]ZnSCH_2C(O)N(\mathbf{H^*})Ph$ ($\mathbf{H^*}$ = H, D) with MeI is characterized by a small normal value of $k_H/k_D = 1.16(1)$ at 0 °C, which is in marked contrast to the substantial inverse (i.e., $k_H/k_D < 1$) value of 0.33 reported for the alkylation of $[Ph(pz^{Bu^t})Bt^{Bu^t}]ZnS[C_6H_4\text{-}o\text{-}N(\mathbf{H^*})C(O)Bu^t]$ by $PhCH_2Br$. Since an observed KIE corresponds to a composite of all steps up to and including the rate determining step, DFT calculations were used to address how the KIE for methylation of $[Tm^{Ph}]ZnSCH_2C(O)N(\mathbf{H^*})Ph$ varies as a function of mechanism. Although the isotope effects for each of the mechanisms considered are predicted to be close to unity at ambient temperature, the only mechanism that is predicted to give rise to a normal KIE is one involving a dissociative step because it involves the formation of $[PhN(H)C(O)CH_2S]^-$ which, as an anion, exhibits a stronger hydrogen bonding interaction than that in $[Tm^{Ph}]ZnSCH_2C(O)N(H)Ph$. On this basis, the reaction

of [Tm^{Ph}]ZnSCH$_2$C(O)N(H)Ph with MeI is proposed to occur via thiolate dissociation rather than direct alkylation of the coordinated thiolate ligand. Correspondingly, mechanisms that involve direct alkylation of coordinated thiolate are predicted to be characterized by $k_H/k_D \leq 1$ because the reaction involves a reduction of the negative charge on sulfur and hence a weakening of the N—H···S hydrogen bonding interaction.

Experimental Procedures

General Considerations. All manipulations were performed using a combination of glovebox, high-vacuum, or Schlenk techniques.[63] Solvents were purified and degassed by standard procedures. ^{1}H NMR chemical shifts are reported in ppm relative to $SiMe_4$ ($\delta = 0$) and were referenced internally with respect to the protio solvent impurity. All coupling constants are reported in Hz. IR spectra were recorded as KBr pellets and are reported in cm^{-1}. Mass spectra were obtained on a Micromass Quadrupole-Time-of-Flight mass spectrometer using an electrospray ion source. [Tm^{Ph}]Li was synthesized as previously reported.[13a] *N*-Phenyl-2-mercaptoacetamide, PhN(H)C(O)CH$_2$SH, was synthesized according to the literature method.[24,64]

Synthesis of [Tm^{Ph}]ZnSCH$_2$C(O)N(H)Ph. A solution of PhN(H)C(O)CH$_2$SH (300 mg, 1.79 mmol) in ethanol (ca. 10 mL) was treated with Li (13 mg, 1.87 mmol), and the mixture was stirred for 1.5 h at room temperature. Zn(NO$_3$)$_2$·6H$_2$O (425 mg, 1.81 mmol) was added, and the mixture was stirred until the compound dissolved. A solution of [Tm^{Ph}]Li (975 mg, 1.79 mmol) in ethanol (20 mL) was added dropwise, thereby resulting in the immediate formation of a cream precipitate. The mixture was stirred for 25 min, and the precipitate was isolated by filtration and dried in vacuo. The product was extracted with chloroform (3 × 10 mL), and the solvent was removed in vacuo to give [Tm^{Ph}]ZnSCH$_2$C(O)N(H)Ph as a cream solid (740 mg, 53.8%). ^{1}H NMR (CDCl$_3$): 3.16 and 3.37 [AB quartet, $^2J_{HH} = 18$ Hz, 2 H of SC*H*$_2$C(O)N(H)Ph], 4.59 [br s, 1 H of *H*B{C$_3$N$_2$H$_2$(Ph)S}$_3$], 6.94 [t, $^3J_{HH} = 8$ Hz, 1 *p*-H of of SCH$_2$C(O)N(H)C$_6$*H*$_5$], 6.98 [d, $^3J_{HH} = 2$ Hz, 3 H of HB{C$_3$N$_2$*H*$_2$(Ph)S}$_3$], 7.07 [d, $^3J_{HH} = 2$ Hz, 3 H of HB{C$_3$N$_2$*H*$_2$-(Ph)S}$_3$], 7.10 [t, $^3J_{HH} = 8$ Hz, 2 *m*-H of SCH$_2$C(O)N(H)C$_6$*H*$_5$], 7.28 [d, $^3J_{HH} = 7$ Hz, 6 *o*-H of HB{C$_3$N$_2$H$_2$(C$_6$*H*$_5$)S}$_3$], 7.34 [d, $^3J_{HH} = 8$ Hz, 2 *o*-H of SCH$_2$C(O)N(H)C$_6$*H*$_5$], 7.37 [t, $^3J_{HH} = 7$ Hz, 3 *p*-H of HB{C$_3$N$_2$H$_2$(C$_6$*H*$_5$)S}$_3$], 7.42 [t, $^3J_{HH} = 7$ Hz, 6 *m*-H of HB{C$_3$N$_2$H$_2$-(C$_6$*H*$_5$)S}$_3$], 9.47 [s, 1 H of SCH$_2$C(O)N(*H*)Ph]. IR data (KBr pellet, cm^{-1}): 3256 ($\nu_{N-H\ stretch}$), 2424 (ν_{B-H}), 1664 (ν_{CO}), 1523 ($\nu_{N-H\ bend}$). Mass spectrum: *m*/*z* (FAB) = 601 {[Tm^{Ph}]Zn}$^+$. Crystals of [Tm^{Ph}]-ZnSCH$_2$C(O)N(H)Ph suitable for single-crystal X-ray diffraction were obtained from both CHCl$_3$ and EtOH solutions, of which the latter were of the composition [Tm^{Ph}]ZnSCH$_2$C(O)N(H)Ph·EtOH due to a hydrogen bonding interaction between ethanol and amide carbonyl oxygen.

Synthesis of [Tm^{Ph}]ZnSCH$_2$C(O)N(D)Ph. In a typical experiment, [Tm^{Ph}]ZnSCH$_2$C(O)N(H)Ph (25 mg, 0.033 mmol) was dissolved in CDCl$_3$ (500 μL) and was treated with MeOH-d_4 (100 μL). Upon standing at room temperature for ~30 min, [Tm^{Ph}]ZnSCH$_2$C(O)N(D)Ph was formed in quantitative yield (>95% deuteration) as indicated by ^{1}H NMR. The volatile components were removed in vacuo to give [Tm^{Ph}]ZnSCH$_2$C(O)N(D)Ph as a solid. IR data (KBr pellet, cm^{-1}): 2432 (ν_{B-H}), 2374 ($\nu_{N-D\ stretch}$), 1656 (ν_{CO}), 908 ($\nu_{N-D\ bend}$).

Table 5. Crystal, Intensity Collection, and Refinement Data

	[Tm^{Ph}]ZnSCH$_2$C-(O)N(H)Ph	[Tm^{Ph}]ZnSCH$_2$C-(O)N(H)Ph1.5EtOH	PhNH(CO)CH$_2$SH
Lattice	triclinic	monoclinic	orthorhombic
Formula	$C_{35}H_{30}BN_7OS_4Zn$	$C_{38}H_{39}BN_7O_{2.5}S_4Zn$	C_8H_9NOS
Fw	769.08	838.18	167.22
space group	$P\bar{1}$	$P2_1/n$	*Ama*2
a/Å	9.990(1)	17.640(1)	9.237(1)
b/Å	10.615(2)	9.864(1)	18.966(2)
c/Å	17.306(2)	25.252(2)	4.603(1)
α/deg	105.875(3)	90	90
β/deg	92.654(3)	110.351(1)	90
γ/deg	96.521(3)	90	90
V/Å^3	1748.0(4)	4119.5(4)	806.4(2)
Z	2	4	4
T/K	243	233	243
radiation λ, Å	0.71073	0.71073	0.71073
ρ (calcd.)/g cm^{-3}	1.461	1.351	1.377
μ (Mo Kα)/mm^{-1}	0.982	0.842	0.338
θ max/deg	28.4	28.3	28.1
no. of data	7750	9471	713
no. of params	451	505	87
R_1	0.0489	0.0402	0.0238
wR2	0.0824	0.0865	0.0663
GOF	1.015	1.009	1.044

Reaction of [Tm^{Ph}]ZnSCH$_2$C(O)N(H)Ph with MeI. A solution of MeI in CDCl$_3$ (0.7 mL, 0.646 M) was added to [Tm^{Ph}]ZnSCH$_2$C(O)N-(H)Ph (10 mg). The reaction was monitored by ^{1}H NMR spectroscopy, which demonstrated the immediate formation of [Tm^{Ph}]ZnI[65] and MeSCH$_2$C(O)N(H)Ph.[66]

Kinetic Isotope Effect for Reaction of [Tm^{Ph}]ZnSCH$_2$C(O)N(H)-Ph and [Tm^{Ph}]ZnSCH$_2$C(O)N(D)Ph with MeI. The KIE for the reaction of [Tm^{Ph}]ZnSCH$_2$C(O)N(H)Ph and [Tm^{Ph}]ZnSCH$_2$C(O)N-(D)Ph with MeI was determined by comparing the rate constants under identical conditions. Specifically, samples of [Tm^{Ph}]ZnSCH$_2$C(O)N-(**H***)Ph and MeI for kinetics experiments were prepared by adding a stock solution of MeI in CDCl$_3$ (0.5 mL of 0.143 M) to [Tm^{Ph}]-ZnSCH$_2$C(O)N(**H***)Ph (2 mg) in a NMR tube that had been cooled to −78 °C, thereby causing the solution to freeze before dissolving [Tm^{Ph}]ZnSCH$_2$C(O)N(**H***)Ph. The sample was allowed to thaw and dissolve before being placed into a NMR spectrometer with a probe temperature of 0 °C. Spectra were acquired every 6 min, and the pseudo-first-order rate constants were determined by a plot of ln[[Tm^{Ph}]-ZnSCH$_2$C(O)N(**H***)Ph] versus time: (i) $k_H = 4.70(2) \times 10^{-5}$ s^{-1} at 0.143 M [MeI]; (ii) $k_D = 4.05(2) \times 10^{-5}$ s^{-1} at 0.143 M [MeI]; and (iii) $k_H/k_D = 1.16(1)$. The individual pseudo-first-order rate constants k_H and k_D were determined from >100 data points to reduce statistical errors. Furthermore, by employing the same stock solution of MeI in CDCl$_3$ to determine k_H and k_D, the error on k_H/k_D is greatly minimized, even though the systematic error on the second-order rate constants may be large.

The concentration dependence for the reaction of [Tm^{Ph}]ZnSCH$_2$C-(O)N(H)Ph with MeI was determined by adding a solution of MeI in CDCl$_3$ (0.6 mL, with concentrations of 0.143, 0.323, 0.646, and 1.24 M) to [Tm^{Ph}]ZnSCH$_2$C(O)N(H)Ph (10 mg) in a NMR tube that had been cooled to −78 °C, thereby causing the solution to freeze before

(63) (a) McNally, J. P.; Leong, V. S.; Cooper, N. J. In *Experimental Organometallic Chemistry*; Wayda, A. L., Darensbourg, M. Y., Eds.; American Chemical Society: Washington, DC, 1987; Ch. 2, pp 6−23. (b) Burger, B. J.; Bercaw, J. E. In *Experimental Organometallic Chemistry*; Wayda, A. L.; Darensbourg, M. Y., Eds.; American Chemical Society: Washington, DC, 1987; Ch. 4, pp 79−98. (c) Shriver, D. F.; Drezdzon, M. A. *The Manipulation of Air-Sensitive Compounds*, 2nd ed.; Wiley-Interscience: New York, 1986.

(64) ^{1}H NMR data for PhN(H)C(O)CH$_2$SH (CDCl$_3$): δ 2.01 [t, $J_{H-H} = 9$ Hz, S*H*], 3.36 [d, $J_{H-H} = 9$ Hz, C*H*$_2$], 7.12 [t, $J_{H-H} = 8$ Hz 1 *p*-H], 7.32 [t, $J_{H-H} = 8$ Hz 2 *m*-H], 7.52 [d, $J_{H-H} = 8$ Hz, 2 *o*-H], 8.52 [br s, N(*H*)]. ^{13}C NMR data (CDCl$_3$): δ 29.12 [t, $J_{C-H} = 141$ Hz, *C*H$_2$], 119.84 [d, $J_{C-H} = 161$ Hz, aryl-*C*H], 124.77 [d, $J_{C-H} = 160$ Hz, *aryl*-*C*H], 129.04 [d, $J_{C-H} = 159$ Hz, aryl-*C*H], 137.27 [s, ipso-*C*], 167.18 [s, *C*(O)].

(65) Kimblin, C.; Bridgewater, B. M.; Churchill, D. G.; Parkin, G. *Chem. Commun.* **1999**, 2301−2302.

(66) MeSCH$_2$C(O)N(H)Ph was prepared by the literature method (ref 36). A solution of NaOH (135 mg, 3.38 mmol) in EtOH (25 mL) was treated with HSCH$_2$C(O)N(H)Ph (150 mg, 1.11 mmol) under a N$_2$ atmosphere. The reaction mixture was stirred for 30 min at room temperature. MeI was added (300 μL, 5.7 mmol), and the reaction was stirred for an additional 45 min at room temperature. The reaction mixture was filtered, and the solvent was removed in vacuo. ^{1}H NMR data for PhN(H)C(O)CH$_2$SCH$_3$ (CDCl$_3$): δ 2.19 [s, SC*H*$_3$], 3.33 [s, C*H*$_2$], 7.12 [t, $J_{H-H} = 8$ Hz 1 *p*-H], 7.33 [t, $J_{H-H} = 8$ Hz 2 *m*-H], 7.55 [d, $J_{H-H} = 8$ Hz, 2 *o*-H], 8.67 [br s, N(*H*)]. ^{13}C NMR data (CDCl$_3$): δ 25.77 [s, *C*H$_2$], 39.21 [s, S*C*H$_3$] 119.71 [s, aryl-*C*H], 124.64 [s, aryl-*C*H], 129.07 [s, aryl-*C*H], 137.30 [s, ipso-*C*], 166.50 [s, *C*(O)].

dissolving [Tm^{Ph}]ZnSCH$_2$C(O)N(H)Ph. The sample was allowed to thaw and dissolve before being placed into a NMR spectrometer with a probe temperature of 0 °C. Spectra were acquired at pre-set time intervals, and the pseudo-first-order rate constants were determined by a plot of ln[[Tm^{Ph}]ZnSCH$_2$C(O)N(**H***)Ph] versus time.

The temperature dependence of the reaction of [Tm^{Ph}]ZnSCH$_2$C(O)N(H)Ph with MeI was determined by adding a solution of MeI in $CDCl_3$ (0.6 mL, 0.646 M) to [Tm^{Ph}]ZnSCH$_2$C(O)N(H)Ph (10 mg) in a NMR tube that had been cooled to −78 °C, thereby causing the solution to freeze before dissolving [Tm^{Ph}]ZnSCH$_2$C(O)N(H)Ph. The sample was allowed to thaw and dissolve before being placed into a NMR spectrometer with a probe temperatures of −20, −10, 0, 10, and 20 °C. Spectra were acquired at pre-set time intervals, and the pseudo-first-order rate constants were determined by a plot of ln[[Tm^{Ph}]ZnSCH$_2$C(O)N(**H***)Ph] versus time.

X-ray Structure Determinations. X-ray diffraction data were collected on a Bruker P4 diffractometer equipped with a SMART CCD detector, and crystal data, data collection, and refinement parameters are summarized in Table 5. The structures were solved using direct methods and standard difference map techniques and were refined by full-matrix least-squares procedures on F^2 with SHELXTL (Version 5.10).[67]

Computational Details. All calculations were carried out using DFT as implemented in the Jaguar suite of ab initio quantum chemistry programs.[68] Geometry optimization calculations were performed with the B3LYP[69] functional employing 6-31G** (H, B, C, N, O, S) and LAV3P (Zn) basis sets.[70] Where appropriate, the energies of the optimized structures were reevaluated by additional single-point calculations on each optimized geometry using the cc-pVTZ(-f)[71] (H, B, C, N, O, S) and LAV3P (Zn) basis sets.[70] Vibrational frequency calculations were performed at the B3LYP level of theory using the basis sets employed for geometry optimization. The transition states {[Tm^{H}]ZnSCH$_2$C(O)N(H)Ph}···MeI}‡ and [PhN(H)C(O)CH$_2$S···Me···I]$^{‡-}$ were verified by stepping along the reaction coordinate and confirming that they transformed into the reactants/products. Cartesian coordinates for the derived geometries and vibrational frequencies are listed in the Supporting Information.

Acknowledgment. We thank the National Institutes of Health (Grant GM46502) for support of this research, and Prof. Mu-Hyun Baik is thanked for obtaining the vibrational frequencies of {[Tm^{H}]ZnSCH$_2$C(O)N(**H***)Ph}···MeI}‡. D.A.Q. was on leave from the State University of New York College at Old Westbury and gratefully acknowledges the UUP Drescher Leave Program.

Supporting Information Available: Kinetics data; Cartesian coordinates and vibrational frequencies for geometry optimized structures; crystallographic data in CIF format for [Tm^{Ph}]ZnSCH$_2$C(O)N(H)Ph, [Tm^{Ph}]ZnSCH$_2$C(O)N(H)Ph·1.5EtOH, and PhN(H)C(O)CH$_2$SH. This material is available free of charge via the Internet at http://pubs.acs.org.

JA0536670

(67) Sheldrick, G. M. SHELXTL, An Integrated System for Solving, Refining and Displaying Crystal Structures from Diffraction Data; University of Göttingen, Göttingen, Germany, 1981.
(68) Jaguar 4.1; Schrödinger Inc.: Portland, OR, 2001. Jaguar 6.0; Schrödinger, Inc.: Portland, OR, 2005.
(69) (a) Slater, J. C. *Quantum Theory of Molecules and Solids, Vol. 4: The Self-Consistent Field for Molecules and Solids*; McGraw-Hill: New York, 1974. (b) Vosko, S. H.; Wilk, L.; Nusair, M. *Can. J. Phys.* **1980**, *58*, 1200−1211. (c) Lee, C. T.; Yang, W. T.; Parr, R. G. *Phys. Rev. B* **1988**, *37*, 785−789. (d) Becke, A. D. *Phys. Rev. A* **1988**, *38*, 3098−3100. (e) Becke, A. D., *J. Chem. Phys.* **1993**, *98*, 5648−5652.
(70) (a) Hay, P. J.; Wadt, W. R. *J. Chem. Phys.* **1985**, *82*, 299−310. (b) Wadt, W. R.; Hay, P. J. *J. Chem. Phys.* **1985**, *82*, 284−298. (c) Hay, P. J.; Wadt, W. R. *J. Chem. Phys.* **1985**, *82*, 270−283.
(71) Dunning, T. H. *J. Chem. Phys.* **1989**, *90*, 1007−1023.